This international standard was developed in accordance with internationally recognized principles on standardization established in the Decision on Principles for the Development of International Standards, Guides and Recommendations issued by the World Trade Organization Technical Barriers to Trade (TBT) Committee.

Designation: E2382 – 04 (Reapproved 2020)

Standard Guide to Scanner and Tip Related Artifacts in Scanning Tunneling Microscopy and Atomic Force Microscopy[1]

This standard is issued under the fixed designation E2382; the number immediately following the designation indicates the year of original adoption or, in the case of revision, the year of last revision. A number in parentheses indicates the year of last reapproval. A superscript epsilon (ε) indicates an editorial change since the last revision or reapproval.

1. Scope

1.1 All microscopes are subject to artifacts. The purpose of this document is to provide a description of commonly observed artifacts in scanning tunneling microscopy (STM) and atomic force microscopy (AFM) relating to probe motion and geometric considerations of the tip and surface interaction, provide literature references of examples and, where possible, to offer an interpretation as to the source of the artifact. Because the scanned probe microscopy field is a burgeoning one, this document is not meant to be comprehensive but rather to serve as a guide to practicing microscopists as to possible pitfalls one may expect. The ability to recognize artifacts should assist in reliable evaluation of instrument operation and in reporting of data.

1.2 A limited set of terms will be defined here. A full description of terminology relating to the description, operation, and calibration of STM and AFM instruments is beyond the scope of this document.

1.3 The values stated in SI units are to be regarded as standard. No other units of measurement are included in this standard.

1.4 *This international standard was developed in accordance with internationally recognized principles on standardization established in the Decision on Principles for the Development of International Standards, Guides and Recommendations issued by the World Trade Organization Technical Barriers to Trade (TBT) Committee.*

2. Referenced Documents

2.1 *ASTM Standards:*[2]

E1813 Practice for Measuring and Reporting Probe Tip Shape in Scanning Probe Microscopy (Withdrawn 2016)[3]

3. Terminology

3.1 *Definitions of Terms Specific to This Standard:*

3.1.1 *artifact*—any feature of an image generated by an AFM or STM that deviates from the true surface. Artifacts can have origins in sample preparation, instrument hardware/software, operation, post processing of data, etc.

3.1.2 *image*—surface topography represented by plotting the z value for feature height as a function of x and y position. Typically the z height value is derived from the necessary z voltage applied to the scanner to allow the feedback value to remain constant during the generation of the image. The "image" is therefore a contour plot of a constant value of the surface property under study (for example, tunneling current in STM or lever deflection in AFM).

3.1.3 *tip*—the physical probe used in either STM or AFM. For STM the tip is made from a conductive metal wire (for example, tungsten or Pt/Ir) while for AFM the tip can be conductive (for example, doped silicon) or non-conductive (for example, silicon nitride). The important performance parameters for tips are the aspect ratio, the radius of curvature, the opening angle, the overall geometrical shape, and the material of which they are made.

3.1.4 *cantilever or lever*—the flexible beam onto which the AFM tip is placed at one end with the other end anchored rigidly to the microscope. The important performance parameters for cantilevers are the force constant (expressed in N/m) and resonance frequency (expressed in kHz typically). These values will depend on the geometry and material properties of the lever.

3.1.5 *scanner*—the device used to position the sample and tip relative to one another. Generally either the tip or sample is scanned in either STM or AFM. The scanners are typically made from piezoelectric ceramics. Tripod scanners use three independent piezo elements to provide motion in x, y, and z. Tube scanners are single element piezo materials that provide coupled x,y,z motion. The important performance parameters

[1] This guide is under the jurisdiction of ASTM Committee E42 on Surface Analysis and is the direct responsibility of Subcommittee E42.14 on STM/AFM.

Current edition approved Dec. 1, 2020. Published December 2020. Originally approved in 2004. Last previous edition approved in 2012 as E2382 – 04 (2012). DOI: 10.1520/E2382-04R20.

[2] For referenced ASTM standards, visit the ASTM website, www.astm.org, or contact ASTM Customer Service at service@astm.org. For *Annual Book of ASTM Standards* volume information, refer to the standard's Document Summary page on the ASTM website.

[3] The last approved version of this historical standard is referenced on www.astm.org.

Copyright © ASTM International, 100 Barr Harbor Drive, PO Box C700, West Conshohocken, PA 19428-2959. United States

Copyright by ASTM Int'l (all rights reserved); Fri Jan 8 20:56:38 EST 2021

for scanners are the distance of movement per applied volt (expressed as nm/V) and the lateral and vertical scan ranges (expressed in microns).

3.1.6 *scan angle*—the angle of rotation of the x scan axis relative to the x-axis of the sample

3.1.7 *tip characterizer*—a special sample used to determine the geometry of the tip. The tip in question is used to image the characterizer. The image then becomes an input to an algorithm for determining the tip geometry.

3.2 *Abbreviations:*

3.2.1 *AFM*—atomic force microscopy (microscope). We refer here to contact mode AFM as opposed to non-contact techniques.

3.2.2 *STM*—scanning tunneling microscopy (microscope).

4. Significance and Use

4.1 This compilation is limited to artifacts observed in scanning tunneling microscopes and contact-mode atomic force microscopes. In particular, this document focuses on artifacts related to probe motion and geometrical considerations of the tip and surface interaction. Many of the artifacts described here extend to other scanned probe microscopies where piezoscanners are used as positioning elements or where tips of similar geometries are used. These are not the only artifacts associated with measurements obtained by STM or AFM. Artifacts can also arise from the following: control electronics (for example, improper feedback gains); noise (mechanical, acoustic, or electronic); drift (thermal or mechanical); problems unique to signal detection methods (for example, laser spillover in optical lever schemes); improper use of image processing (real time or post processed); sample preparation, environment (for example, humidity) and tip-surface interaction (for example, excessive electrostatic, adhesive, shear, and compressive forces). It is suggested that these other types of artifacts form the basis of future ASTM guides.

5. Artifacts in STM and AFM

5.1 *Artifacts arising from Scanner Motion*—Scanners are made from piezoelectric ceramic materials used to accurately position the tip relative to the surface on the nanometer scale. They exhibit an inverse piezoelectric effect where the material will undergo dimensional change in an applied electric field. Ideal behavior is often assumed when using these devices in STM or AFM microscopes. Ideal behavior implies: (*1*) linear response in dimensional change per applied volt; (*2*) no dependence of the dimensional response on the direction of the voltage change, the magnitude of the voltage change, or the rate of the voltage change (Fig. 1). The motions of these devices are subject to deviations that include non-linearity, hysteresis, and creep (**1-5**).[4] In addition to these non-ideal motions which are characteristic of independent scanner axes, artifacts may arise as a consequence of coupling between the axes.

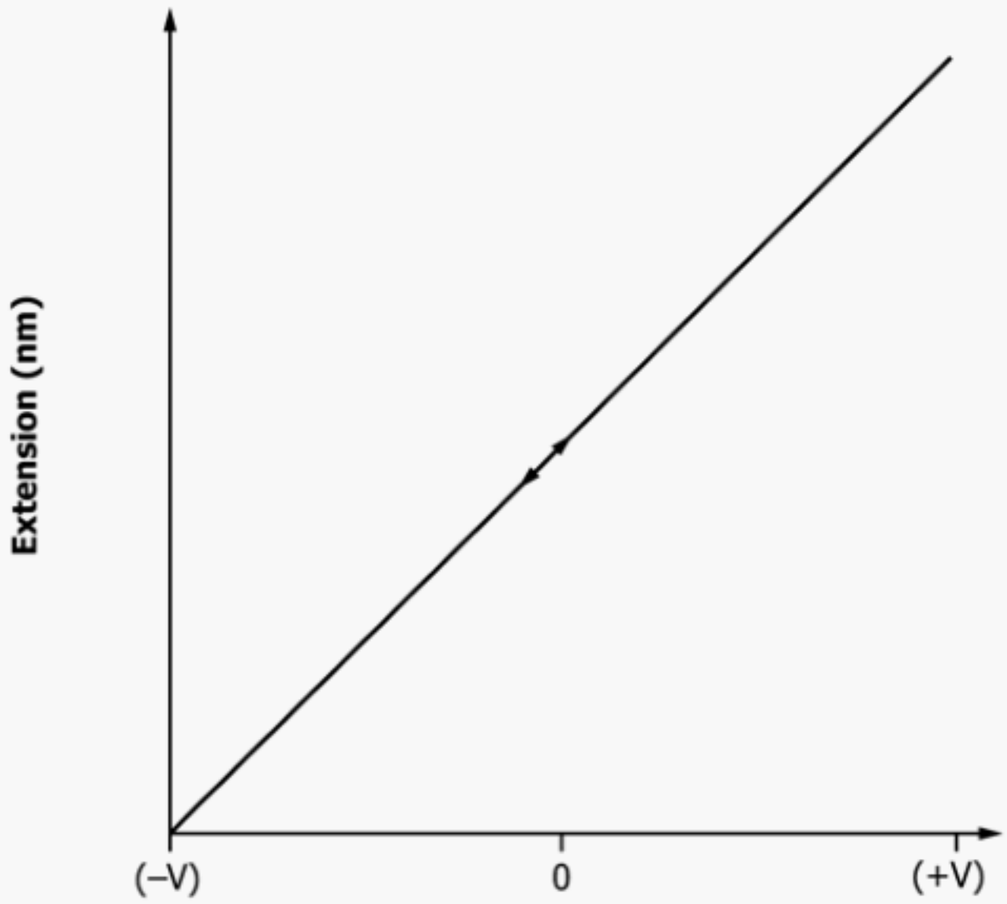

FIG. 1 Ideal Behavior of a Piezoelectric Scanner in One Dimension (Either *x*, *y*, or *z*)

5.1.1 *Non-Linearity*—Non-linearity means that the response of the scanner in nm/V changes as a function of applied voltage. Typically the response deviates more at larger positive or negative voltages than near zero applied volts (**2**) (Fig. 2). Non-linear effects in the lateral direction (x,y) can be observed most clearly when scanning a periodic structure with known spatial frequencies such as a diffraction grating. Since the scanner does not move linearly with applied voltage, the measurement points will not be equally spaced. The observed spacings will vary over the image and some linear features will appear curved. While obvious for test structures, this effect could go unnoticed on other samples that do not have evenly spaced surface features. This effect can be compensated for in software by applying a non-linear voltage ramp during scanning based on prior calibration (open loop method) or by independently measuring the position of the scanner using an additional position sensor such as a capacitor plate (closed loop method) (**5**). An example of the open loop correction method is given in Fig. 3. Non-linear effects in z or height measurements are less obvious but can be detected using vertical height standards (**4**). They are most noticeable when trying to measure small features (small changes in V) and large features (large changes in V) within the same scan. They are also more difficult to correct for due to the complex coupling of motion of x and y to z, in say, a tube scanner.

5.1.2 *Hysteresis*—Hysteresis occurs in piezoelectric materials when the response traces a different path depending on the direction of the voltage change (Fig. 2). The magnitude of the effect will depend on the DC starting voltage, the size of the voltage change, the rate of the voltage change, and the scan angle. The effects of hysteresis can be compensated for by means of a software correction. However, the accuracy of the correction is limited by the need to create a model with a large number of variables. In the case where voltage ramps are applied to the scanners, such as in rastering in x,y for STM or

[4] The boldface numbers in parentheses refer to a list of references at the end of this standard.

Copyright by ASTM Int'l (all rights reserved); Fri Jan 8 20:56:38 EST 2021

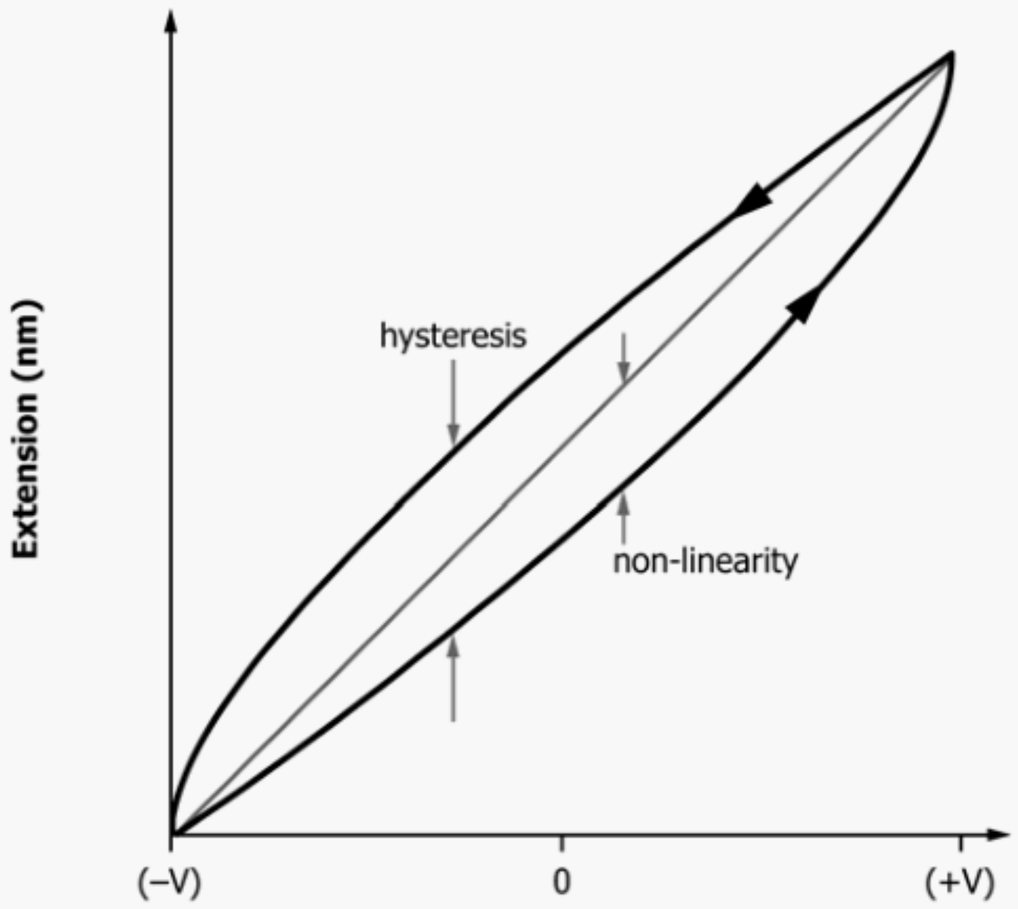

NOTE 1—Non-linear extension in response to linear applied voltage and hysteresis where the sensitivity varies depending on direction of applied voltage.

FIG. 2 Non-Ideal Behavior in a Piezoelectric Scanner

AFM imaging or for ramping in z for generating a force versus distance curve in AFM, the tip or sample will move non-uniformly. Hysteresis could explain why the distance between the same features in an image might differ depending on the direction of scan (trace versus retrace), the size of the scan, or the rate at which the tip is scanned. It would also explain inaccuracies in step heights of large features where large voltage sweeps are necessary in the z direction (**5**).

5.1.3 *Creep*—Creep describes the continued motion of the scanner after a rapid change in voltage, such as might occur when the scanner encounters a large step during scanning. The tube will continue to move even if the voltage remains fixed or changes sign. This is a time dependent effect and its magnitude will depend on the size of the voltage change and the rate of voltage change (Fig. 4). Creep accounts for the initial lateral drift apparent after zooming or moving to a new area which will settle out after several scan lines have been recorded (Fig. 5a). Creep accounts for the overshoot and slopes at both the plateaus and bases in line profiles of periodic, tall features that have been recorded at a fast scan rate. It is also very noticeable in generating AFM force versus distance curves where the x and y scans are disabled and the z element voltage is ramped. Both hysteresis and creep account for the higher force seen in the unloading versus loading portion of the curves for the same sample displacement (so called "reverse-path" effect (**3**)) seen in Fig. 5b.

5.1.4 *Dynamic Range*—The maximum extension of a piezoceramic scanner in x, y, or z will depend on the response of the piezo material, the size and shape of the scanner, and the maximum voltages that can be applied to the piezo electrodes. Each scanner has a stated range of x, y, and z motion. Features in an image can appear clipped if the vertical height exceeds the available range of z motion prescribed for the scanner in use. If the sample plane is substantially tilted relative to the scanner, portions of the image may appear to go flat as the scanner is contracted or elongated to its dynamic range limit. This is most often a concern with long range scanners that may have lateral to vertical range ratios in excess of 10:1.

5.1.5 *Coupled Motion:*

5.1.5.1 *Bowing*—In either tube or tripod scanners the z motion is coupled to x and y motion. For a tube scanner this results in the tube moving in an arc as the tube bends in x or y directions during scanning. If uncorrected this can give the appearance of bowing (a central dip) in an otherwise flat sample. Some systems correct for this in real time by using a line by line planefit of the data. Alternatively a polynomial plane can be fit to and subtracted from the data set after image capture. As with dynamic range effects the bowing artifact is more common for long range scanners.

5.1.5.2 *Abbe Offset Error*—Another artifact related to coupled motion is the Abbe offset error. When the point of interest on the sample surface is displaced from the true measuring system (that is, the undeflected scanner tube z-axis), an angular error exists in the positioning system and, therefore, the measured displacement. The magnitude of this error is directly proportional to the length of the 'lever arm' times the angular offset in radians. In a scanned sample configuration the lever length is estimated by the sum of the tube length plus the distance to the sample surface. This sum is typically tens of millimeters while the scanning displacement is only a few microns so the angular offsets are typically <<0.0001 (radians). A good example of this effect is in the measurement of lattice spacings in cleaved mica using a short tube scanner in contact mode (**6**). As the sample height is increased the measured lattice spacings decrease for the same xy scan size.

5.1.6 *Ringing*—Ringing occurs when the feedback amplifier gain or filter frequency is too high. This causes the tube to oscillate or ring at high frequency and the image becomes dominated by noise. In extreme cases the ringing is audible. Sometimes optimum imaging occurs with PID settings set just below the onset of ringing, however, once other parameters are changed, for example, scan speed or size, the ringing may return. Horizontal ringing is responsible for the turnaround effect at image edges where the scanner reverses direction during scanning.

5.2 *Artifacts Caused by the Tip*—Artifacts derived from the STM or AFM probe tip is the most common sort of artifact observed with scanned probe microscopes. Consideration of the geometry and shape, material of construction, and the possible presence of structural defects and contamination, assists in recognizing tip artifacts. The heights and depths of major surface features determine what portion of the tip interacts with the surface (and therefore which portion of the tip needs to be considered as a source of artifacts). Fig. 6 shows an idealized tip characterized by an opening half-angle, α (α = 30° in the example), an aspect ratio (length to base width (L/W = 1 in the example), and a spherical shape at the apex. The spherical tip described in Fig. 6 is idealized and one of many possible or real descriptions of actual tips.

Table 1 summarizes the important performance parameters for STM and AFM tips commercially available at this time. A

Copyright by ASTM Int'l (all rights reserved); Fri Jan 8 20:56:38 EST 2021

TABLE 1 Important Parameters of Commercially Available Tips

Type	General Use	Material	Gross Shape	Aspect Ratio[A] (half angle)	Nominal Radius of curvature of tip (nm)
pyramidal silicon nitride	AFM	Si_3N_4 (nominal)	square-based pyramid	0.7:1 (35°)	<= 40 nm
oxide sharpened silicon nitride	AFM	Si_3N_4 (nominal)	square- based pyramid[B]	0.7:1 (<35°[B])	<= 20 nm
etched silicon	AFM	Si	kite shaped[C]	3:1 (17° or 10°/25°)[C]	<= 10 nm
ion-milled silicon nitride	AFM	Si_3N_4 (nominal)	Conical[D]	5:1 (5°)	<= 10 nm
e-beam deposited tip	AFM, STM	ill-defined; mostly carbon	Conical[E]	>10:1 (2-3°)	<= 5 nm
electrochemically etched wire	STM	W, Au, or Pt Pt/Ir alloy	Conical	~5:1 (8-10°)	<= 50 nm
ion-milled wire	STM	Pt/Ir alloy	Conical	~5:1 (5°)	<= 5 nm
mechanically cut wire	STM	Pt/Ir alloy	Ill-defined	Asperity[F]	<= 50 nm (variable)

[A] The aspect ratio is defined as the ratio of L_{tip}:W_{tip} as shown in Fig. 6.
[B] A cusp is introduced at the outer 0.1 micron that results in a sharper point and correspondingly smaller half angle.
[C] Due to the "kite" shaped cross-section the half angle is symmetric from side to side and asymmetric from front to back on the shank. At the tip the cross-section is triangular.
[D] Produced by focused ion-beam (FIB) milling of conventional pyramidal silicon nitride tip.
[E] Produced by e-beam deposition of contamination on the apex of a conventional pyramidal silicon nitride tip in an SEM or FEGSEM.
[F] Due to the nature of the cutting, a nanoscale asperity is formed which is responsible for the imaging

detailed description of analytical tip shapes and the means by which the shape of real tips may be characterized is available in Practice E1813.

The nominal characteristics of commercially available tips must be considered in order to begin to interpret the resulting AFM or STM image (**7**). As a dramatic example consider the case where an AFM tip scans a surface which has an array of protruding features which are "sharper" than the scanning tip (Fig. 7a). The resulting image will contain images of the tip (b,c) and not the surface features. Here, the features of the specimen protruded more than 2 microns above the surface with a radius of curvature smaller than the pyramidal AFM tip used to scan the surface. The features were tall enough to scan not only the tip but also part of the cantilever on which the tip was deposited. It is even possible to see the angle that the cantilever makes with the surface in the image (c). Note also that when the specimen scans the probe tip, the displayed image is a 3-axis inversion of the physical orientation of the tip in space. That is, x maps to –x, y maps to –y, and z maps to –z. This is an extreme example of the geometrical mixing effect that goes on between the tip and sample surface (**8**). Many times the effect is much more subtle. Specific instances of this mixing are described below:

5.2.1 *Geometric Mixing of the Tip Shape and Surface Features*—The geometric mixing of the tip and surface is non-linear in nature. The apex of the tip is not always the contact point with the surface. The closest or proximal point determines the tip's height. This point is not necessarily the apex but can be on the shank or even the cantilever itself (**9, 10**). In the general case with tip, T, and sample, S, of arbitrary shape, the image, I, is given (**11, 12**) by

$$I = S\ [oplus]\ (-T) \tag{1}$$

Here the $\oplus$ symbol represents the dilation operation from mathematical morphology, a detailed definition of which is contained in the references.

5.2.1.1 *Broadening of Surface Features*—One commonly encountered consequence of this dilation is most evident when AFM or STM tips are used to scan features that have radii of curvature similar to or smaller than that of the tip. This might be the case when trying to image a biomolecule fixed to a smooth substrate (**13**) or imaging grain structure in columnar thin films (**14**). Fig. 8 illustrates the situation. The radius of curvature, R_t, of the idealized spherical tip is slightly larger than that of the radius of curvature, R_s, of the idealized spherical surface feature. Assuming that neither the tip nor surface feature deforms during imaging, the height of the surface feature is accurately represented while its width, W_{image}, is broadened. The broadening can be calculated geometrically and is found to be:

$$W_{image} = 4(R_t \times R_s) \tag{2}$$

This is a special case of Eq 1 applied to a spherical tip and surface feature. Other special cases of interest; when the tip and surface feature are either both spherical (as in Fig. 8) or both parabolic ($y = \pm 0.5x^2/r$) the radius of the resulting image is the sum of the radii of the surface and tip (**10**).

$$R_i = R_t + R_s \tag{3}$$

Here the R_x are to be understood as the unsigned magnitudes of the image, tip, and sample radii. When the tip and surface feature have rectangular cross sections a similar relation holds, except that the widths are summed instead of the radii.

5.2.1.2 *Imaging Undercut Surface Feature*—The non-linear mixing of the tip and surface feature is also readily evident when imaging steep-walled structures or undercuts. In these cases the sidewall angle of the surface feature is greater than that of the tip shank. A schematic is shown in Fig. 9. In this case the sidewalls of the image of the surface feature contain information about the shanks of the tip used to scan it. In the resulting image, the base of the surface feature is increased by a term depending on the opening half-angles of the tip (which

Copyright by ASTM Int'l (all rights reserved); Fri Jan 8 20:56:38 EST 2021

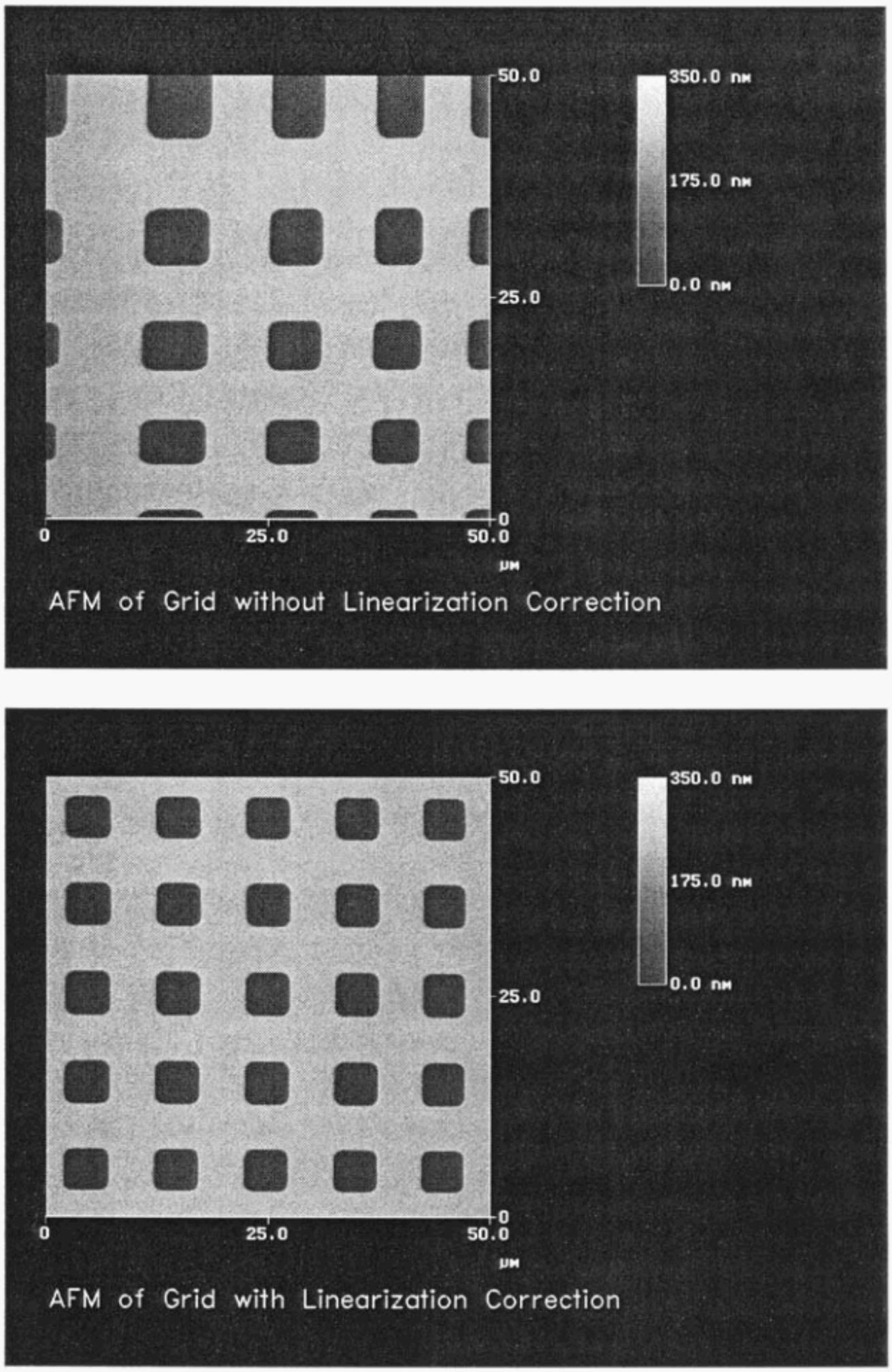

NOTE 1—(Images courtesy of G. Meyers. Used with permission of The Dow Chemical Company.)

FIG. 3 AFM of a Two-Dimensional Grating (Top) without Software Linearity Correction and (Bottom) with the Open-Loop Correction

may or may not be symmetric), and the height of the feature. The measured width at the top of the feature will be broadened by the tip radius as described above. In Fig. 10, AFM images of a polymeric membrane support reproduce the surface features observed in a field emission SEM micrograph taken at the same magnification. However, this is not the case when comparing the AFM and SEM images of the membrane surface. The convoluted or folded nature of the morphology seen in the SEM image is not at all reproduced in the AFM image because the re-entrant features are necessarily hidden.

5.2.1.3 *Imaging Pores, Trenches, and Holes*—Similar arguments can be made for geometric mixing of the tip shape when imaging surface features that have negative excursions from the mean surface plane such as pores, trenches and holes. In these cases, however, the mixing can lead to a reduction in size of the surface feature.

When the tip scans a pore with a diameter that is close to the diameter of the tip, the tip cannot move fully into the pore due to contact with the pore edges. This is shown schematically in Fig. 11. For a spherical tip the depth the tip can penetrate into the pore has a quadratic dependence on the pore diameter, D, for depths less than the radius of curvature of the tip, R_t. As the tip cannot fully penetrate into the pore a false bottom is reached. This artifact makes it difficult to size small pores or

Copyright by ASTM Int'l (all rights reserved); Fri Jan 8 20:56:38 EST 2021

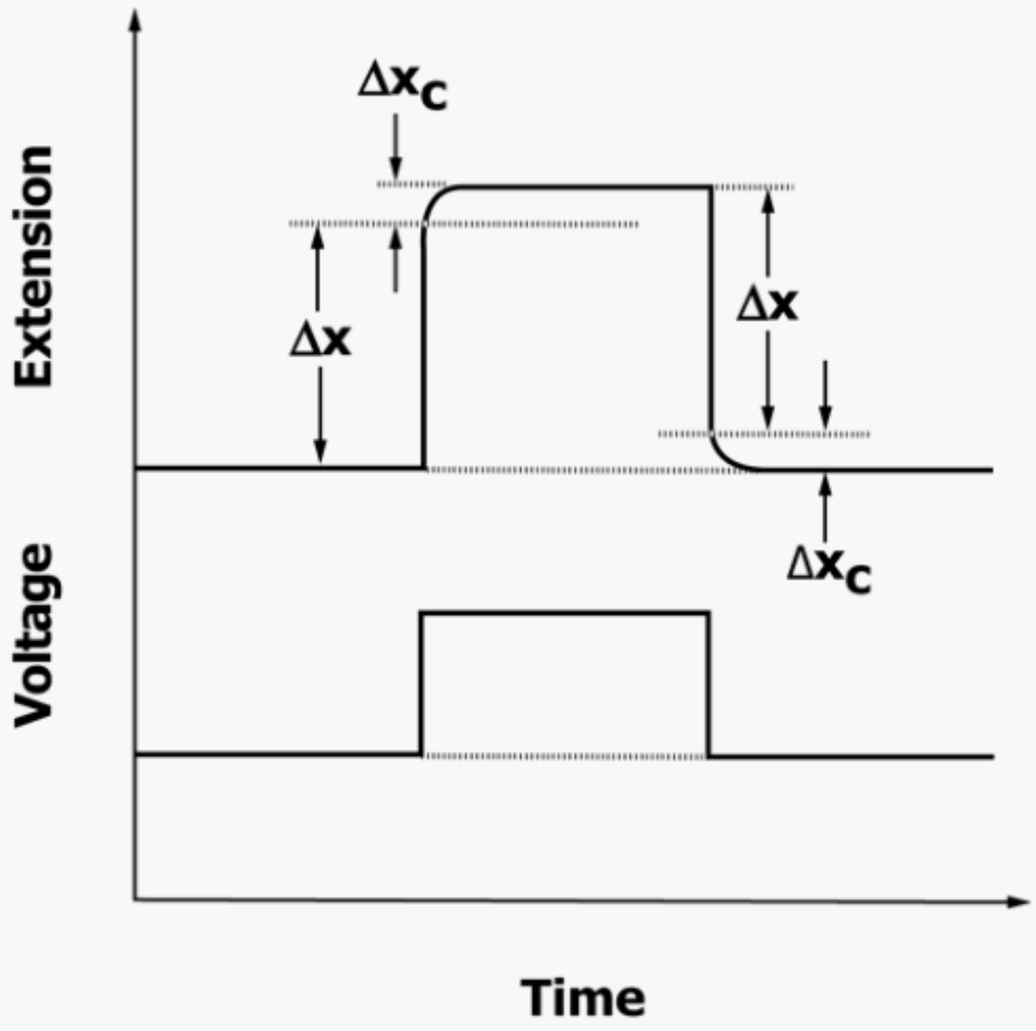

NOTE 1—The scanner exhibits a delay in response to sudden voltage changes (used with permission from ThermoMicroscopes, now Veeco Instruments, Inc.).

FIG. 4 Creep in a Piezoelectric Scanner is Another Non-Ideal Behavior

even to distinguish a true pore from a small surface depression. Fig. 11 illustrates this artifact. A more subtle consequence of this effect occurs when the surface under study is made up of a close-packed array of features with radii of curvature smaller than the tip. Because the holes between features are recorded as narrow cusps, the Fourier transform of the images may contain frequency components that are physically unreal (**5**, **15**, **16**).

Geometrical mixing of the tip with larger structures such as trenches or vias that are closer in size to the entire tip introduces sidewall artifacts. This is shown schematically in Fig. 12. The apparent width of the trench is smaller than the actual width because the shank of the tip is imaged by both sidewalls of the trench.

Other common situations are noteworthy. If the width of the trench is smaller than the base width of the tip and the trench is deeper than the tip is long, the tip will be unable to access the bottom of the trench and will bottom out (Fig. 13). If the width of the trench exceeds the base diameter of the tip and the trench is again deeper than the tip is long, the image will reflect a false flat bottom because the cantilever itself will now limit the excursion of the tip into the trench (Fig. 14). A good example of the latter case is shown in Fig. 15 where a tip was used to scan a microhardness indent on a steel surface. The apparent flat bottom is an artifact.

5.2.1.4 *Missing Information or Regions of Inaccessibility*—A consequence of the geometric mixing of the tip shape with the real surface structure is that the resulting image may contain areas where structural information about the original surface is missing (**7**, **9**, **10**, **17**, **18**). Consider the undercut surface feature mentioned previously. If there is a second feature in the vicinity of the undercut the tip may not see it. In Fig. 16, the apparent sidewall of the taller feature has completely hidden the shorter bump. The image sidewall only contains information about the tip shank and cannot indicate whether or not a shorter bump is present. For this reason the description of the mixing as a "convolution" of tip and surface shape is not rigorously correct. If this were true it should then be possible to "deconvolve" the original surface from the image if, for example, the tip shape was known exactly. In the example of Fig. 16, any attempt to regain the original surface profile from the image profile and actual tip profile would not regenerate the second, smaller feature. Consideration of these regions of inaccessibility of surface features is of utmost importance in attempting to describe the information content of an AFM or STM image.

5.2.1.5 *Angular Effects*—The schematics to this point have assumed that the scanning tip z-axis is normal to the surface plane under study. For practical reasons, cantilevers are mounted in many commercial instruments so that the tip z-axis is tilted 10° to 15° off normal. The microscopist need only adjust his interpretation of potential mixing problems to take this into account. As an example, consider the undercut feature described in Fig. 9. If the tip axis is now rotated 10 degrees off surface normal a new mixing situation occurs as shown in Fig. 17.

5.2.1.6 *Axial Symmetry Effects*—Commercially available tips that have conical cross-sections include electrochemically etched STM tips, e-beam evaporated STM and AFM tips, and ion-milled STM or AFM tips. These tips nominally have axially symmetric opening half-angles. Silicon nitride tips used for AFM have a square based pyramid geometry. As such the opening half-angle depends on whether one is considering the face to face angle or edge to edge angle. Etched silicon tips have symmetric half-angles in one direction and asymmetric half-angles in the other. When measuring critical dimensions that could involve geometrical mixing of the shank of the tip with the real surface (for example, when measuring sidewall slopes of microlithographic features), it is important to be aware of the nominal shape of the tip in use. If the sample is rotated, its features will sample different sides of the tip. For tips that are not axially symmetric, the half angle may change significantly. Opening half-angles for some of the more commonly available AFM and STM tip types are given in Table 1.

5.2.2 *Non-Ideal Tips*—Actual tips, of course, do not have geometrically idealized shapes. Defects can be intrinsic to the tip, that is, part of the manufacturing process, or extrinsic, that is, develop during use. Common intrinsic defects include wedge shapes for square based pyramidal silicon nitride tips or double tips for oxide etched silicon nitride tips. Current manufacturing processes have improved such that these types of defects are generally rare. In all cases use of these tips leads to distortions in the resulting image because they introduce new and unexpected geometries which deviate from the ideal (**7**). Fig. 18 provides some examples from an STM placed inside an SEM where the tip could be characterized after it had scanned a test surface. The figure shows the STM image and an SEM image of the tip used to produce the STM image. Fig. 19 shows some examples of intrinsic defects found on commercially available silicon nitride AFM tips. Fig. 20 compares the

Copyright by ASTM Int'l (all rights reserved); Fri Jan 8 20:56:38 EST 2021

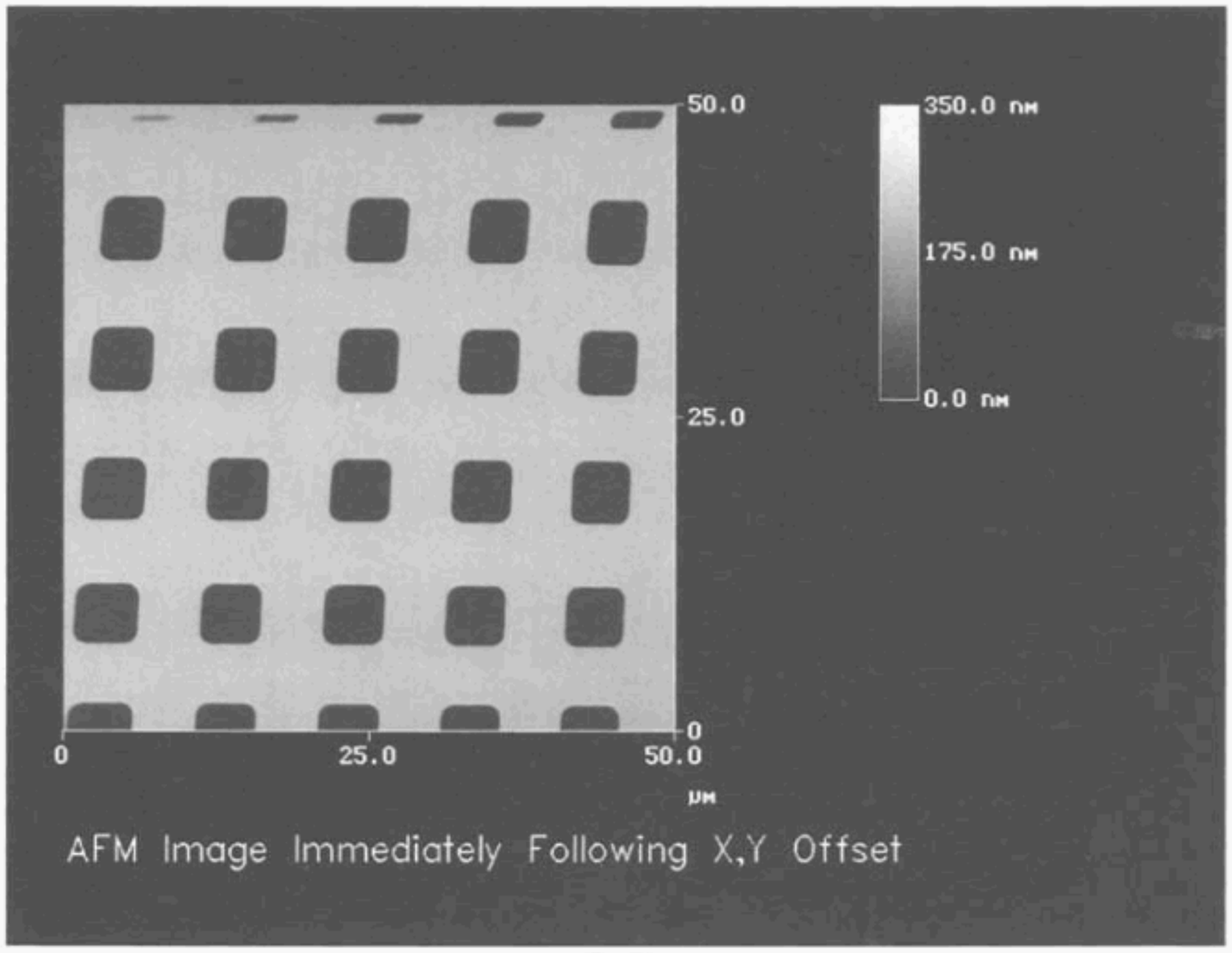

(a)

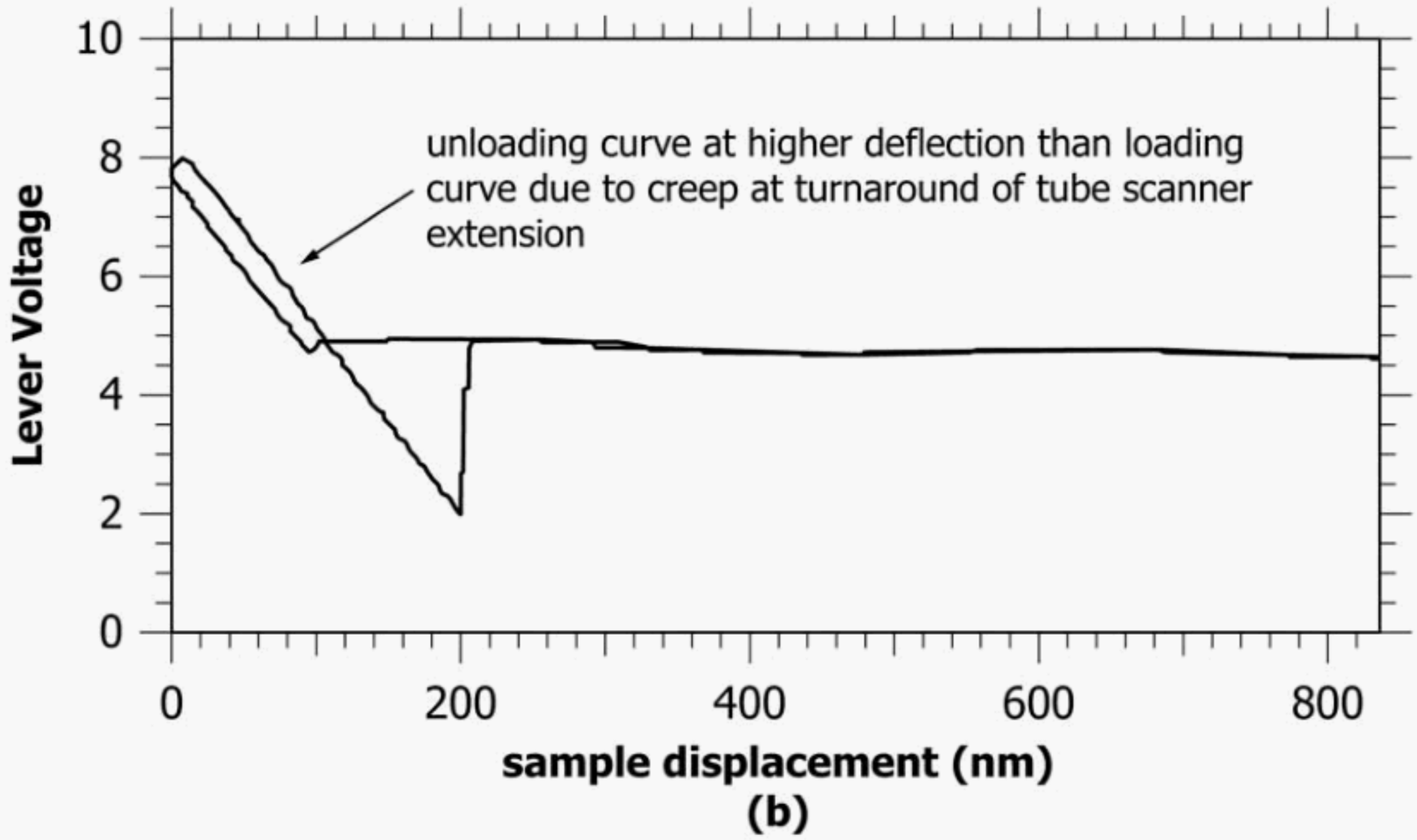

(b)

NOTE 1—In (*a*) creep is seen in the *x, y* direction after a rapid offset in *x* and was applied during imaging of a two-dimensional grating. In (*b*) creep and hysteresis are seen in the *z* direction for a single force versus distance curve. (Image and graph courtesy of G. Meyers. Used with permission of The Dow Chemical Company.)

FIG. 5 Examples of Creep and Hysteresis in Piezoelectric Scanner

contact mode AFM images of an ion sputtered ceramic surface using a good tip and a multiple tip. The latter provides a "ghosted" appearance. Multiple tips can develop during scanning due to wear and it is possible to see the "ghosting" occur in the middle of scan.

5.2.3 *Contamination of Tips*—Tips may become contaminated or damaged during use. If the tip picks up debris from the surface the geometry of the tip has now changed and so the way in which the tip shape mixes will also change and lead to new distortions in the image. Similarly, if the tip wears during scanning its geometry may change, leading to new distortions. In Fig. 21, a silicon nitride tip used for contact mode AFM gave images which were reproducible in the up scan direction but different from the reproducible images obtained in the down

Copyright by ASTM Int'l (all rights reserved); Fri Jan 8 20:56:38 EST 2021

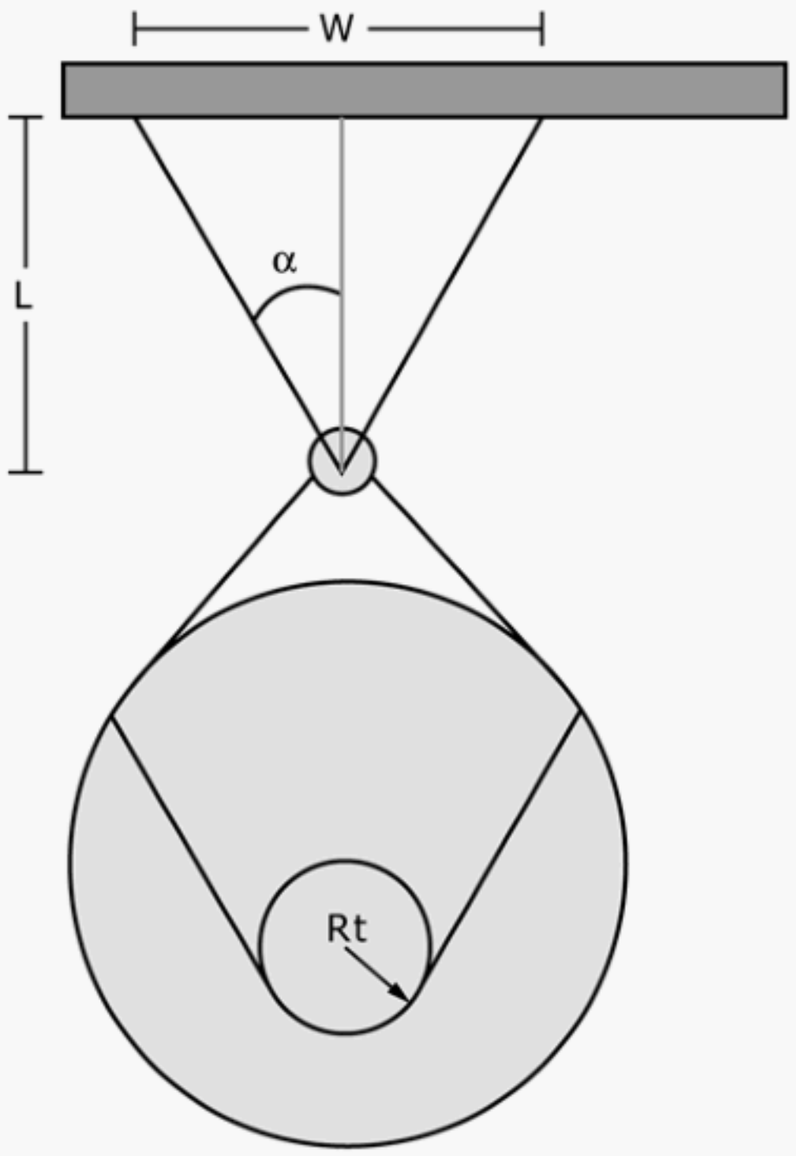

FIG. 6 Important Parameters for an Idealized Conical Tip with Spherical End Radius

scan direction. The nature of this distortion was found to be extrinsic contamination. Solvent cleaning of the tip was found to restore the symmetry between up and down scan images.

5.2.4 *Approaches to the Mixing Problem— Tip Shape Reconstruction*—Much progress has been made in understanding the geometric mixing problem.

Many workers have suggested using special cases of the broadening effect described in 5.2.1.1 to determine information about a tip by imaging small features with known, regular cross-sections. This approach includes the use of colloidal gold particles (**19**, **20**), latex spheres (**21**), starburst polymers (**22**), and rod-shaped biomolecules (**13**). Some tip shapes (for example, parabolic (**13**)) have been treated explicitly. Of course, real tips may not conform to the idealized geometry, and any defects also contribute to the profiles (**20**).

More general approaches use tip characterizers of any known geometry (**11**, **12**, **18**, **23-27**). An AFM or STM image of the structure is collected. From the image and modeled geometry of the characterizer, an outer bound on the tip and its orientation relative to the surface can be determined. Characterizers of different sizes may be used to sample only the tip apex or both the tip apex and tip shank. With the knowledge of the real tip shape and orientation, the image of a sample can be processed to remove many of the tip artifacts, thereby producing an improved estimate of the sample geometry. Because some information may be missing from the image (as described in 5.2.1.4) such a reconstruction does not necessarily completely restore the original surface. In principle it is possible to ascertain which areas are completely restored and which are not (**18**, **11**). However, at present these "certainty maps" are strongly sensitive to noise in the image (**12**).

Another means of tip shape reconstruction is the "blind" method where the shape of the tip can be estimated from the image data even when the exact shape of the surface or characterizer is not known independently (**11**, **12**, **27-29**). The reconstruction relies on the fact that some tips are inconsistent with an observed image. For example, one may rule out tips that are more blunt than observed bumps on the surface. The actual tip must be consistent with all the observed image features. This method provides an outer bound on the tip geometry. For well-chosen characterizers the outer bound should be a good estimate of the tip shape. When conditions for both apply, for example when a tip characterizer contains both known and unknown regions, it may be possible to combine the blind method with the known characterizer method of the last paragraph (**12**, **29**).

6. Keywords

6.1 Abbe offset error; creep; dilation; hysteresis; nonlinearity; probe-sample mixing; AFM; STM; tip shape; proximal probe; geometric mixing; image reconstruction

Copyright by ASTM Int'l (all rights reserved); Fri Jan 8 20:56:38 EST 2021

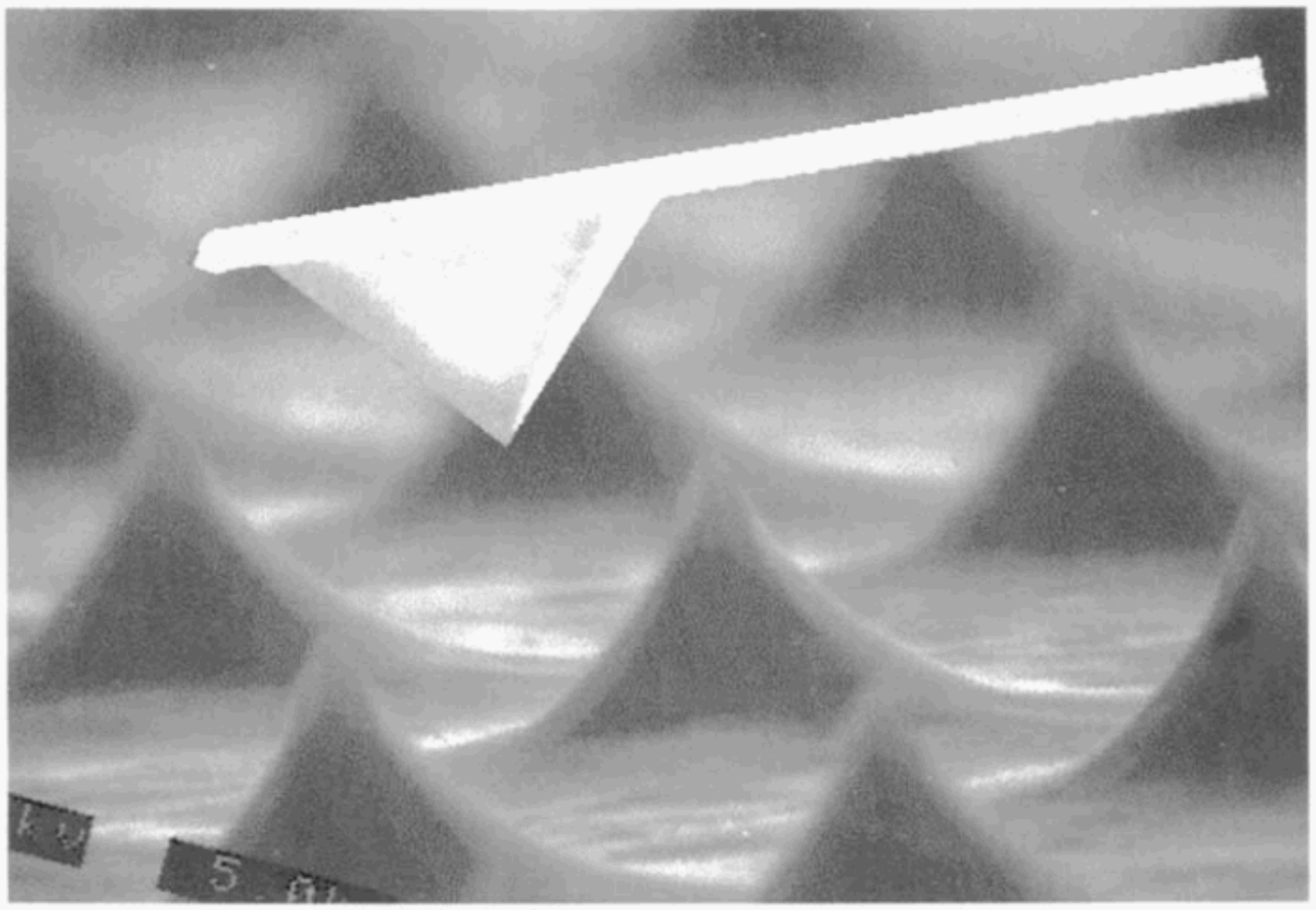

(a) Si field emitter array with AFM tip (insert)

NOTE 1—In the array the emitters are located on a square grid with a 10 micron pitch. A FEGSEM image of an AFM cantilever/tip is inset. The cantilever is tilted 10° to simulate its position in the microscope. The emitter tips are longer and sharper than the AFM tip. (FEGSEM images courtesy of D. Millbrant. Used with permission of The Dow Chemical Company. The Si emitter sample was provided by H. Busta of Amoco.)

FIG. 7 FEGSEM Image of a Silicon Field Emitter Array (Sample Tilted 85°)

Copyright by ASTM Int'l (all rights reserved); Fri Jan 8 20:56:38 EST 2021

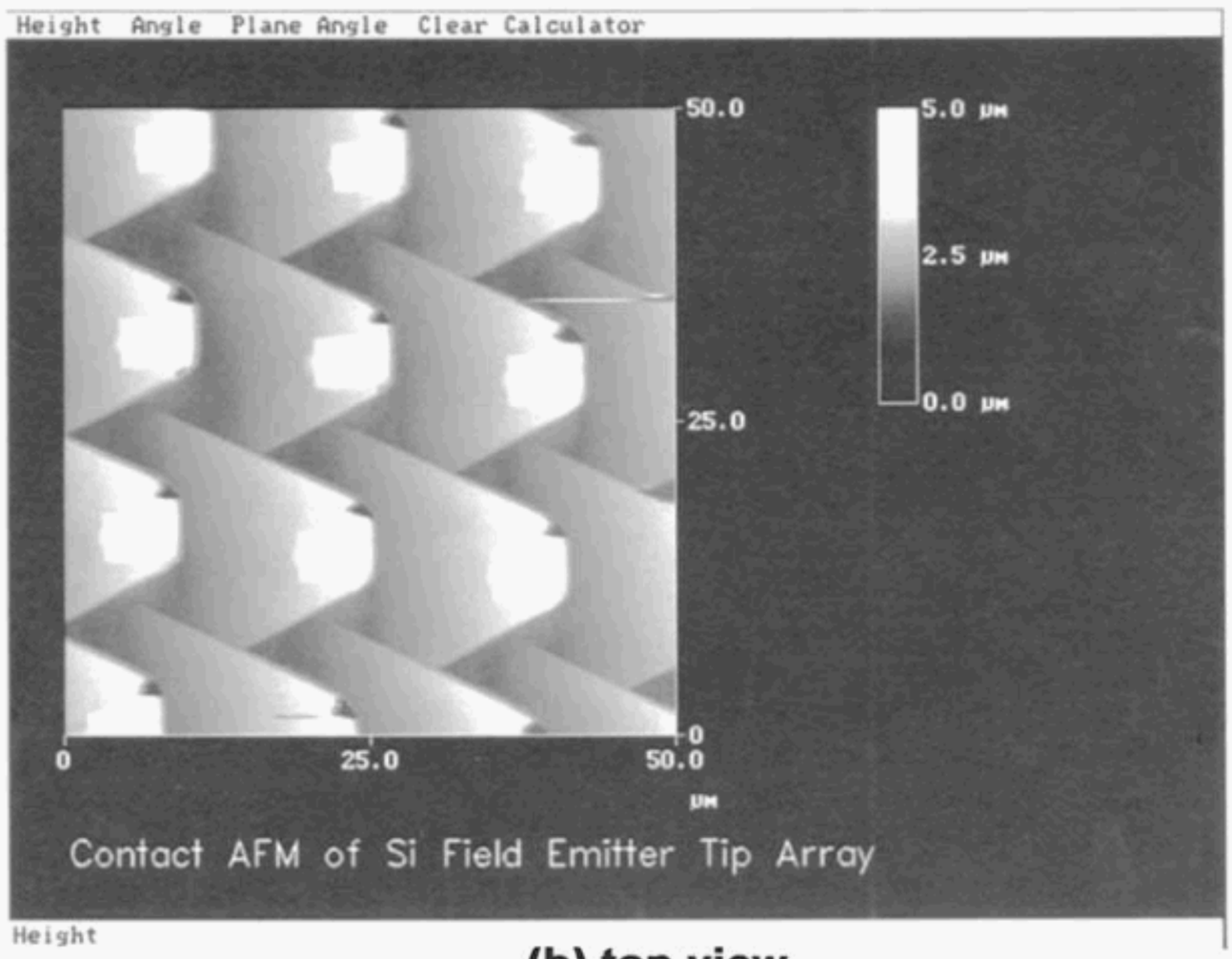

(b) top view

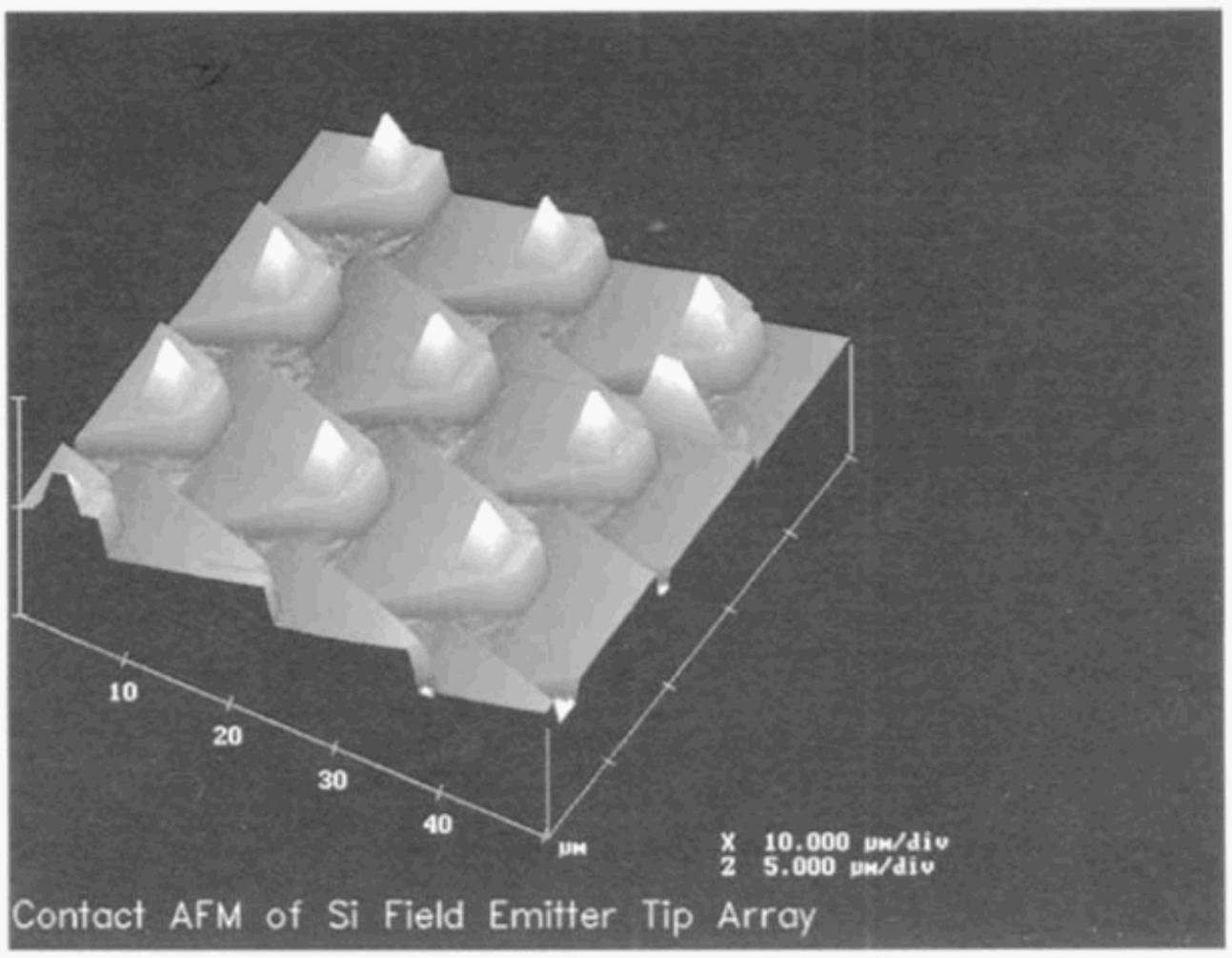

(c)perspective view

NOTE 1—(AFM images by D.Chernoff. Used with permission of Advanced Surface Microscopy.)

FIG. 7 AFM Images Resulting from the Tip Encountering an Array of Surface Features which are Sharper than the Scanning Tip
(continued)

Copyright by ASTM Int'l (all rights reserved); Fri Jan 8 20:56:38 EST 2021

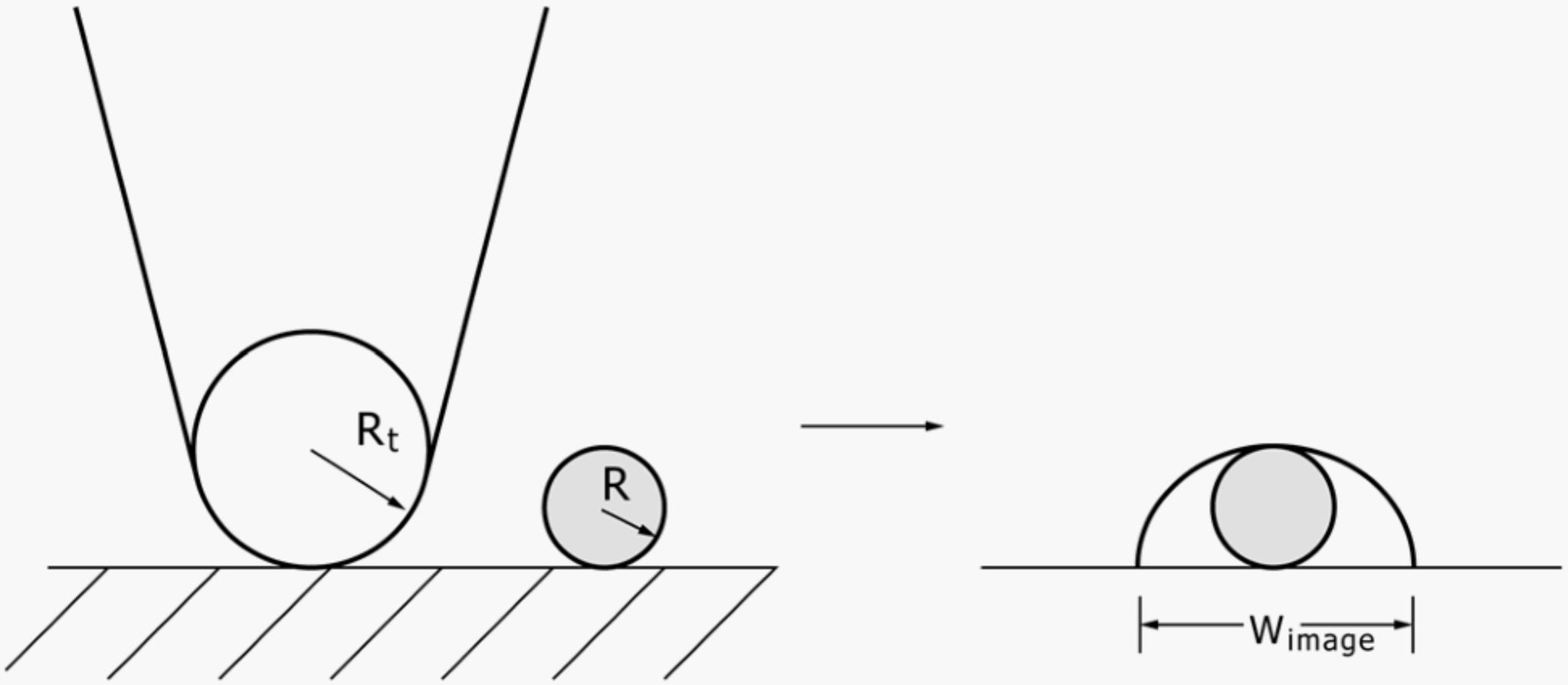

FIG. 8 Schematic of Tip Broadening Effect for an Idealized Spherical Tip (Radius R_t) and Spherical Surface Feature (Radius R_s)

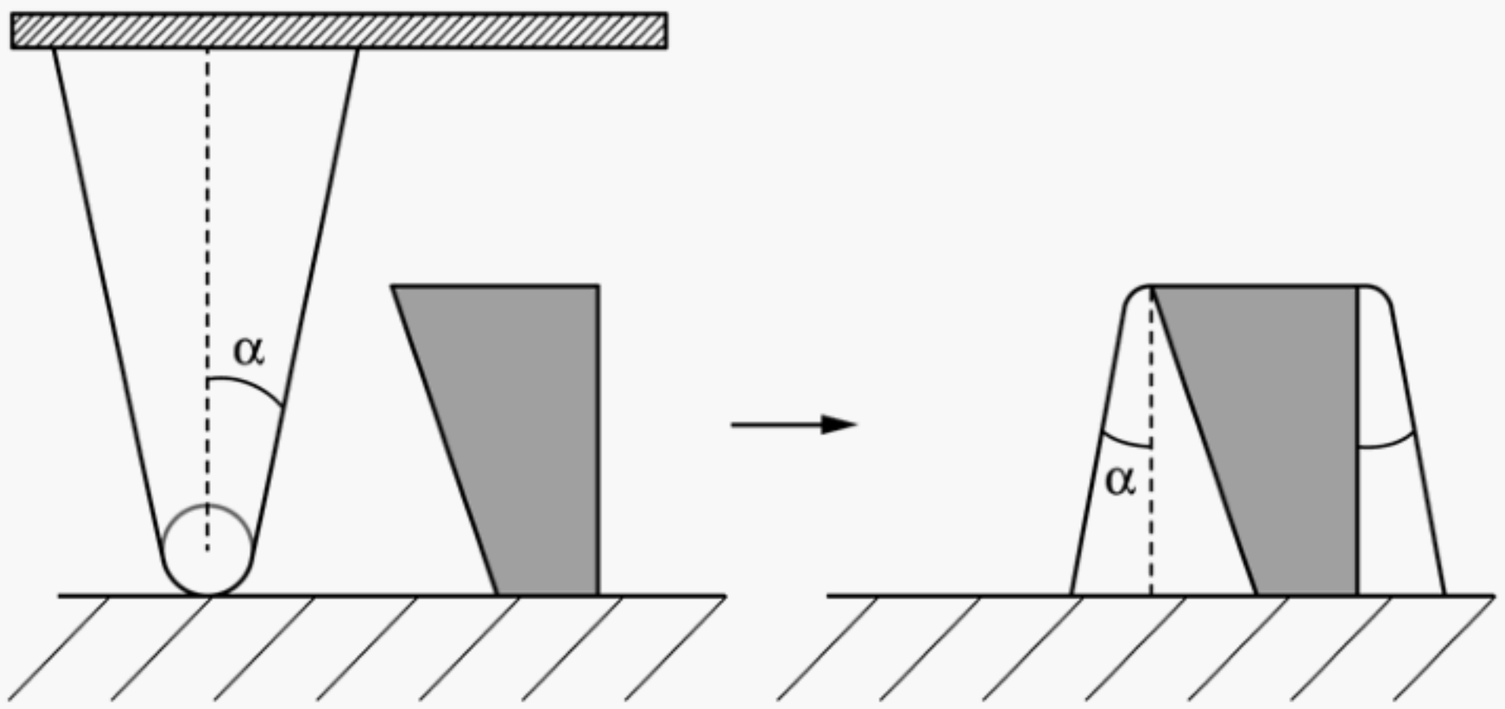

NOTE 1—The resulting image has sidewalls that are profiles of the tip and not the original surface feature.

FIG. 9 Schematic of Tip Broadening Effect Due to a Surface Feature which is Undercut

Copyright by ASTM Int'l (all rights reserved); Fri Jan 8 20:56:38 EST 2021

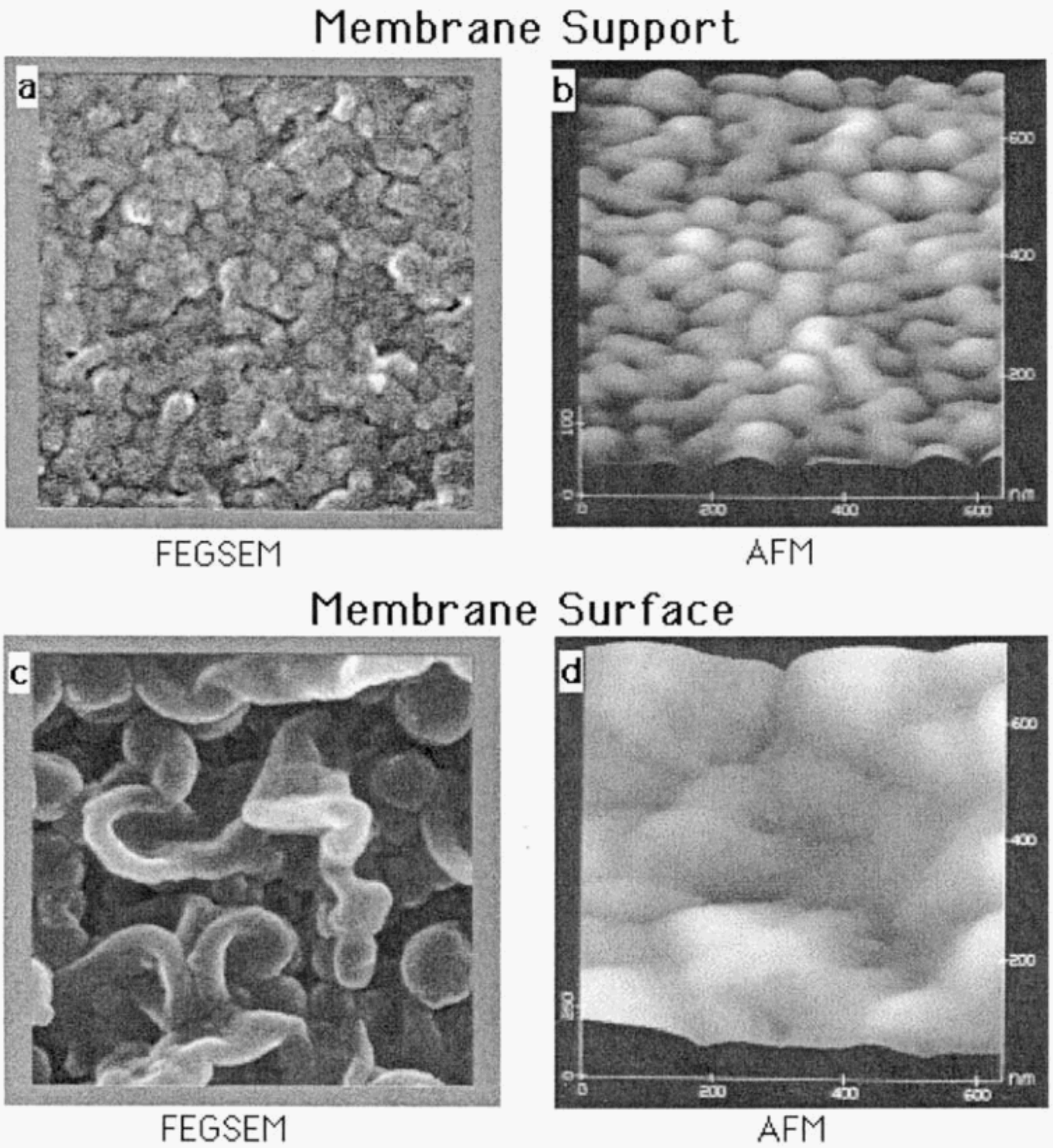

NOTE 1—Aside from some broadening of features the AFM image of the membrane support reproduces the features of the SEM image at similar magnification (compare ***a*** to ***b***). The SEM of the surface of the membrane is convoluted and undercut. The AFM image is not representative of the actual surface imaged (compare ***c*** to ***d***). (SEM images courtesy of J. Marshall and AFM images courtesy of G. Meyers. Used with permission of The Dow Chemical Company.)

FIG. 10 An Example of the Artifact Described in Fig. 9

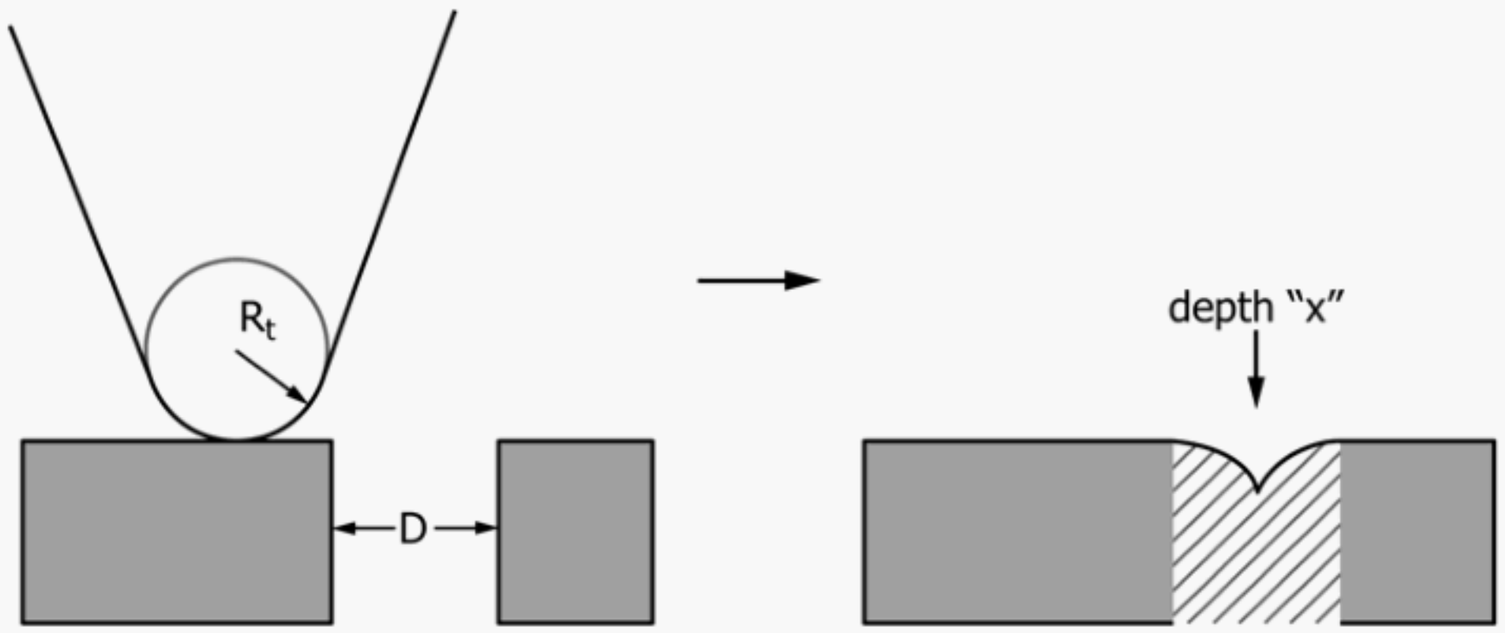

NOTE 1—For a spherical tip shape the depth of penetration has a quadratic dependence on the pore's initial width and the tip radius.

FIG. 11 Schematic of the Pore Size Reduction Effect Due to Contact Proximity of the Pore's Side Walls

Copyright by ASTM Int'l (all rights reserved); Fri Jan 8 20:56:38 EST 2021

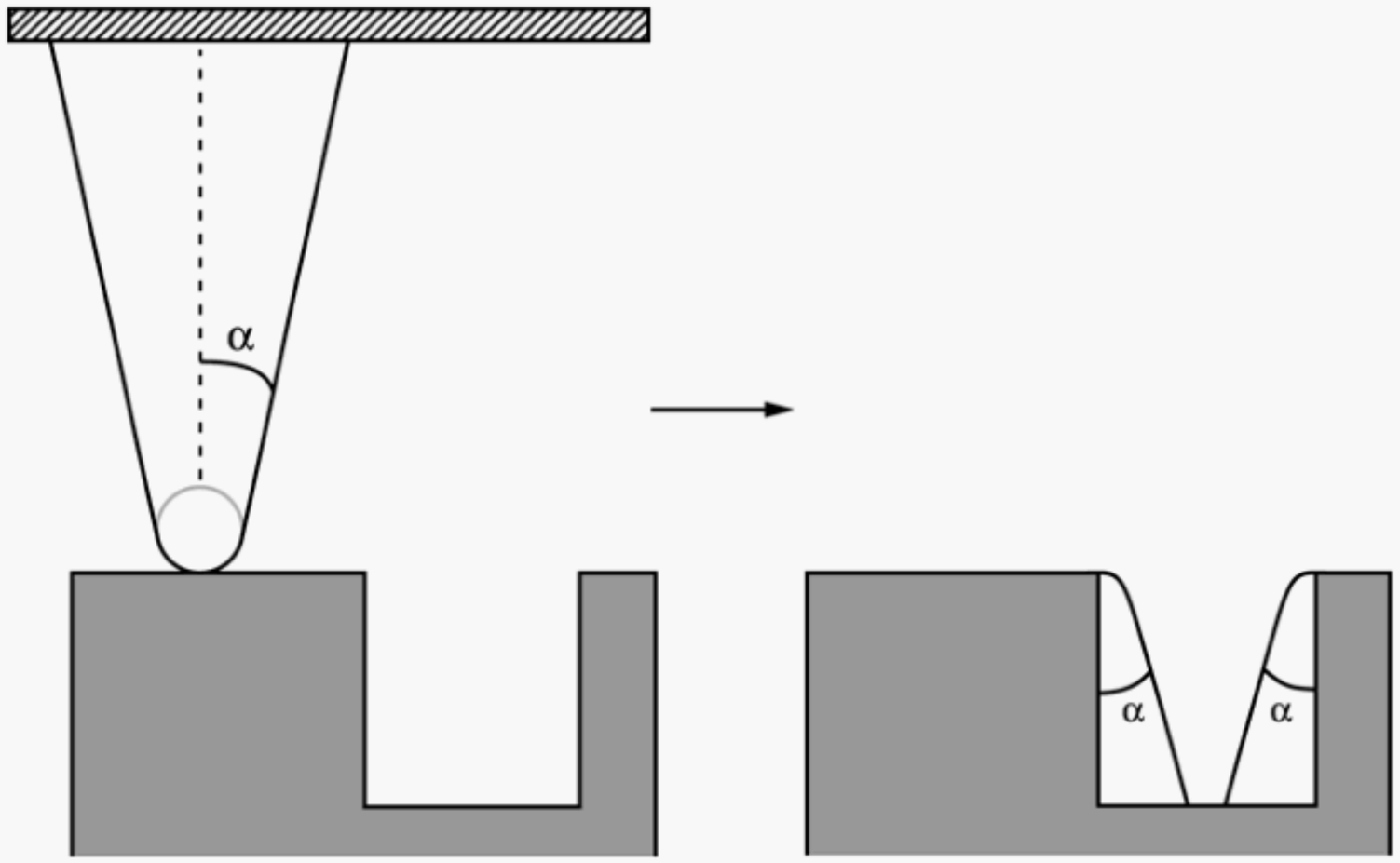

FIG. 12 Schematic of the Trench Width Reduction Effect

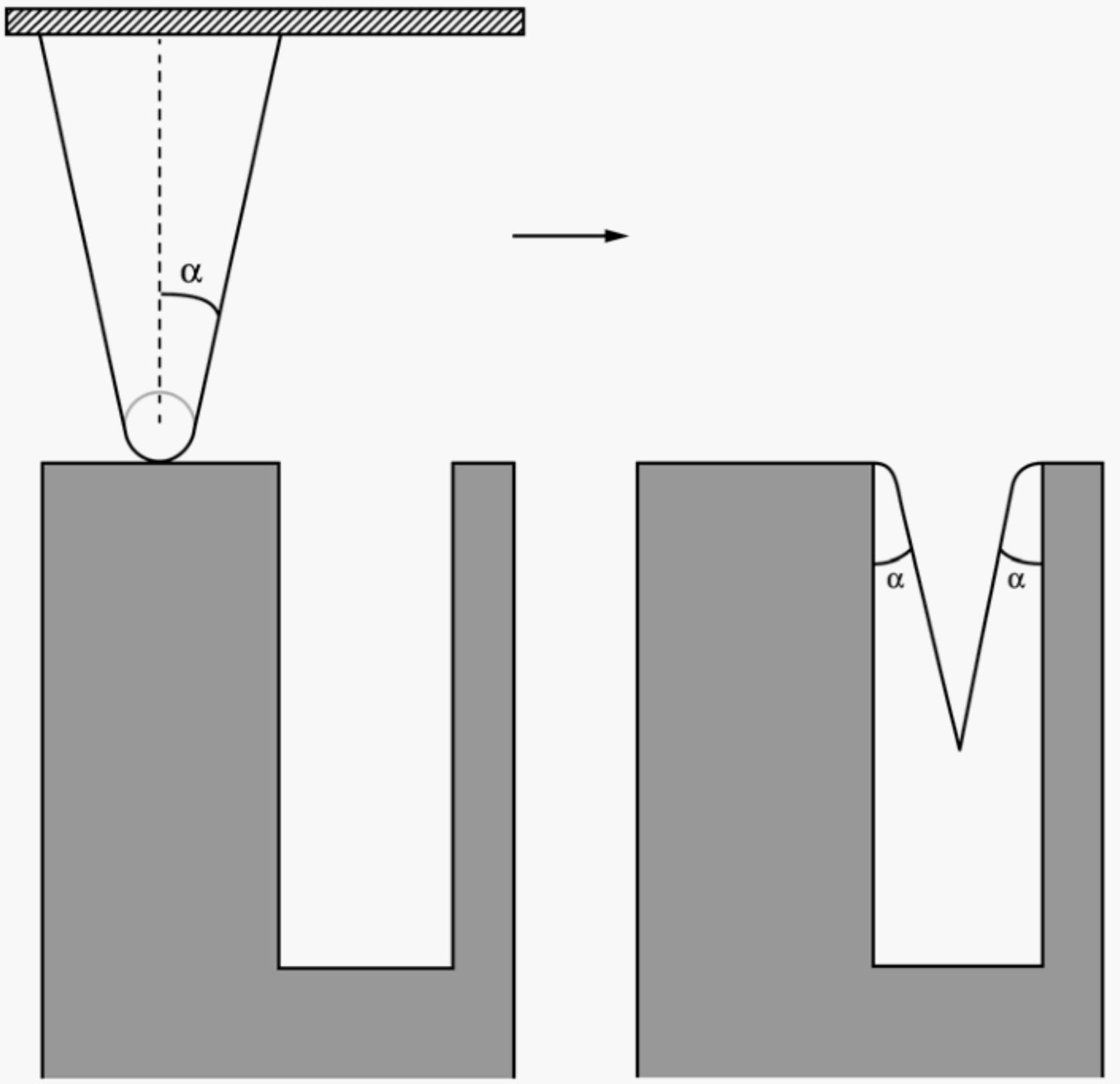

NOTE 1—A flat bottom is never seen.

FIG. 13 Schematic of Tip Bottoming Out Effect Due to Contact of Trench Sidewalls with Tip Shank

Copyright by ASTM Int'l (all rights reserved); Fri Jan 8 20:56:38 EST 2021

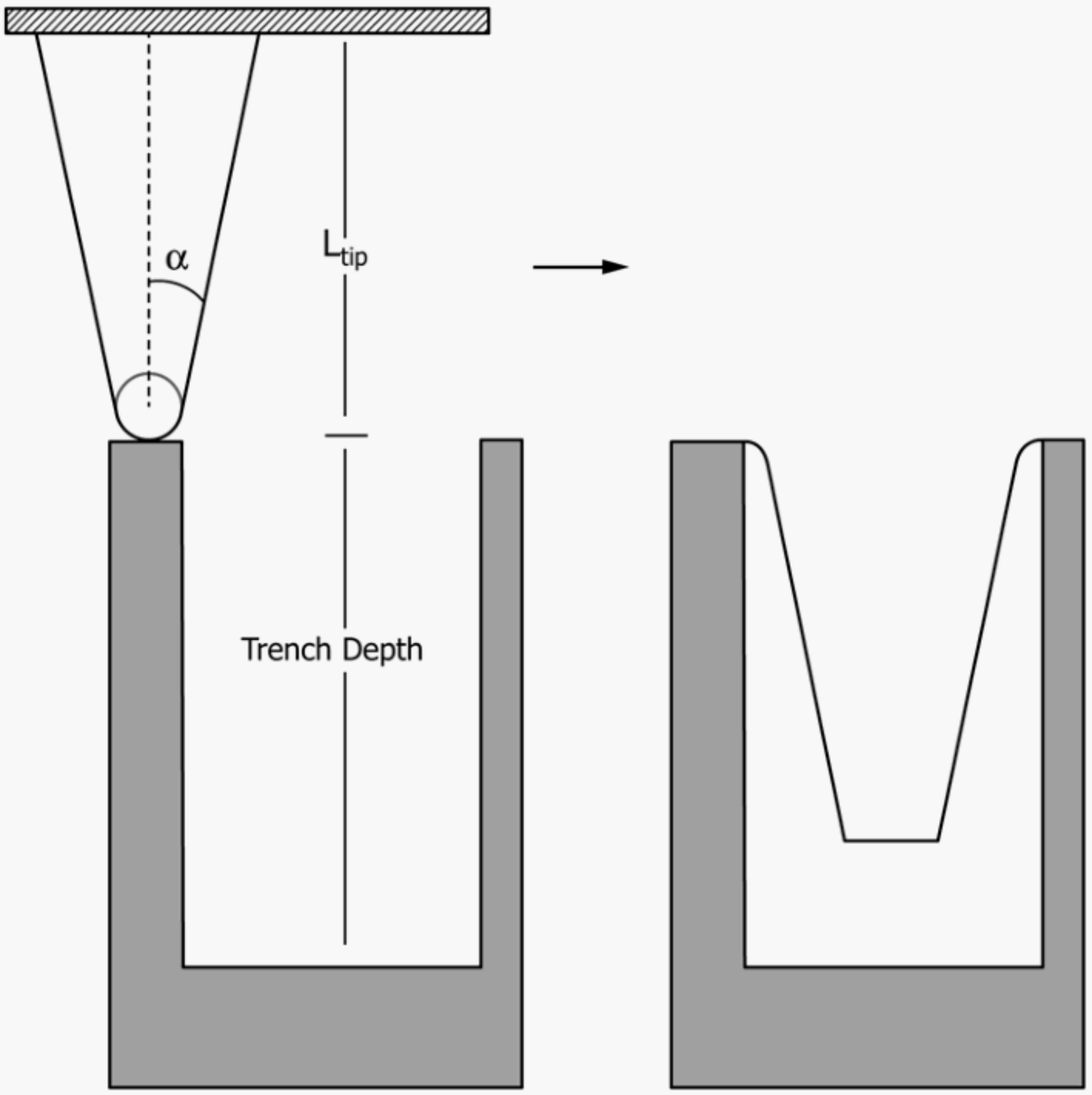

NOTE 1—An apparent flat bottom is seen but is not the real bottom of the trench.

FIG. 14 Schematic of Tip Bottoming Out Effect due to Contact of the Cantilever with the Surface of a Deep Trench

Copyright by ASTM Int'l (all rights reserved); Fri Jan 8 20:56:38 EST 2021

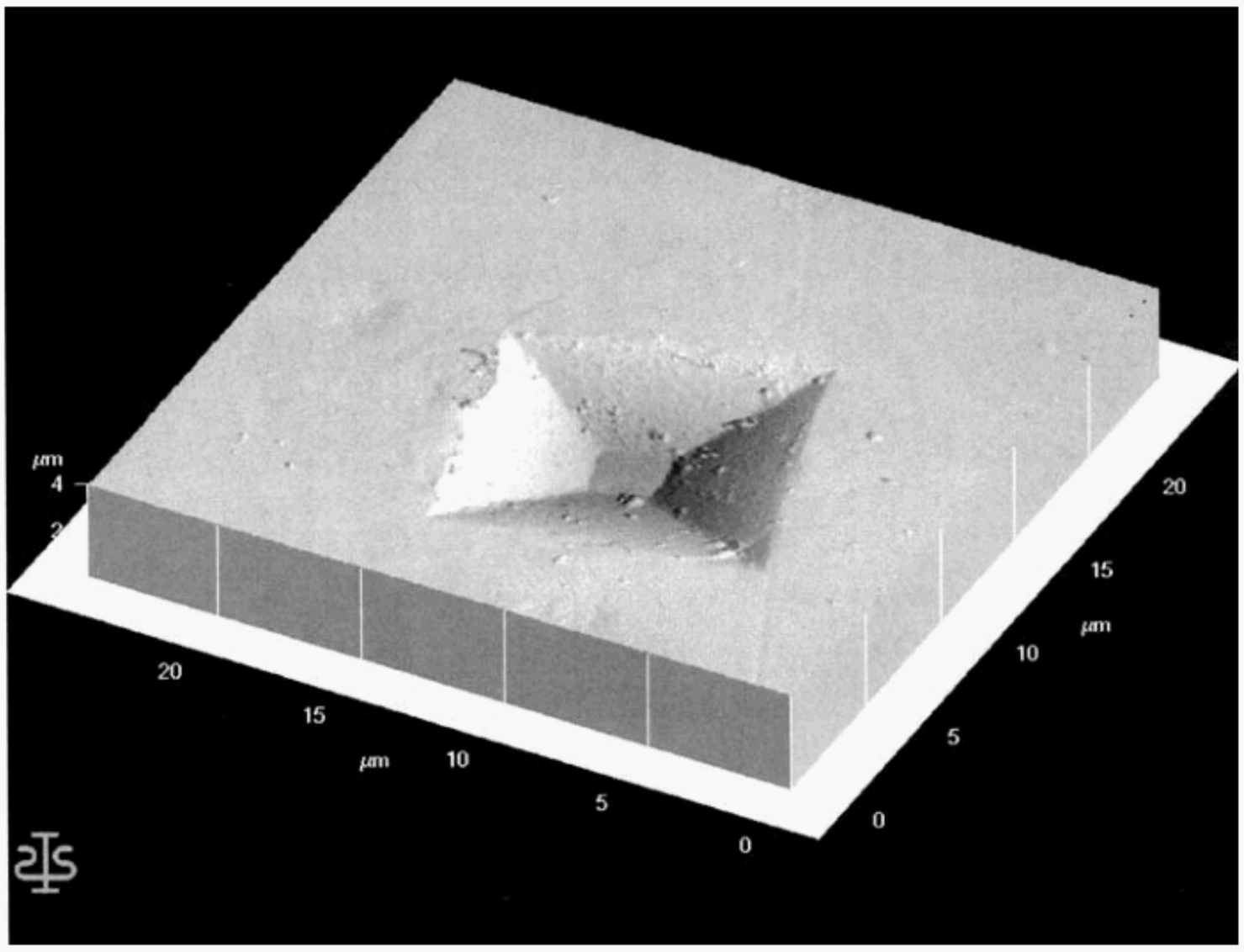

NOTE 1—An apparent flat bottom is seen at the base of a microhardness indent in 440C stainless steel surface using contact mode AFM (image courtesy of P. Abel, NASA-Lewis Research Center, Cleveland, OH).

FIG. 15 An Example of the Artifact Described in Fig. 14

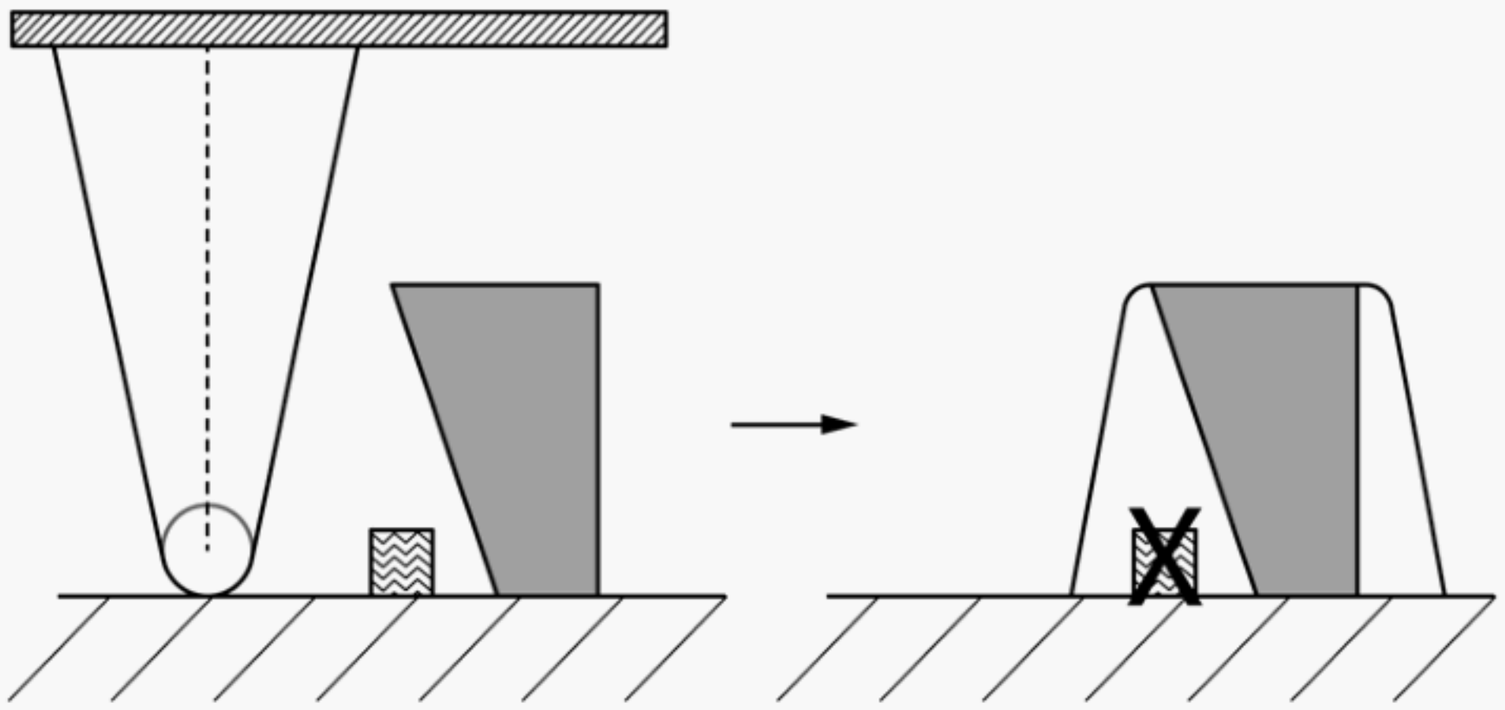

NOTE 1—In this case the small square feature would not be imaged although it is part of the actual surface.

FIG. 16 Regions of Surface Inaccessibility Result from Geometrical Mixing of Tip Shape and Surface Features

Copyright by ASTM Int'l (all rights reserved); Fri Jan 8 20:56:38 EST 2021

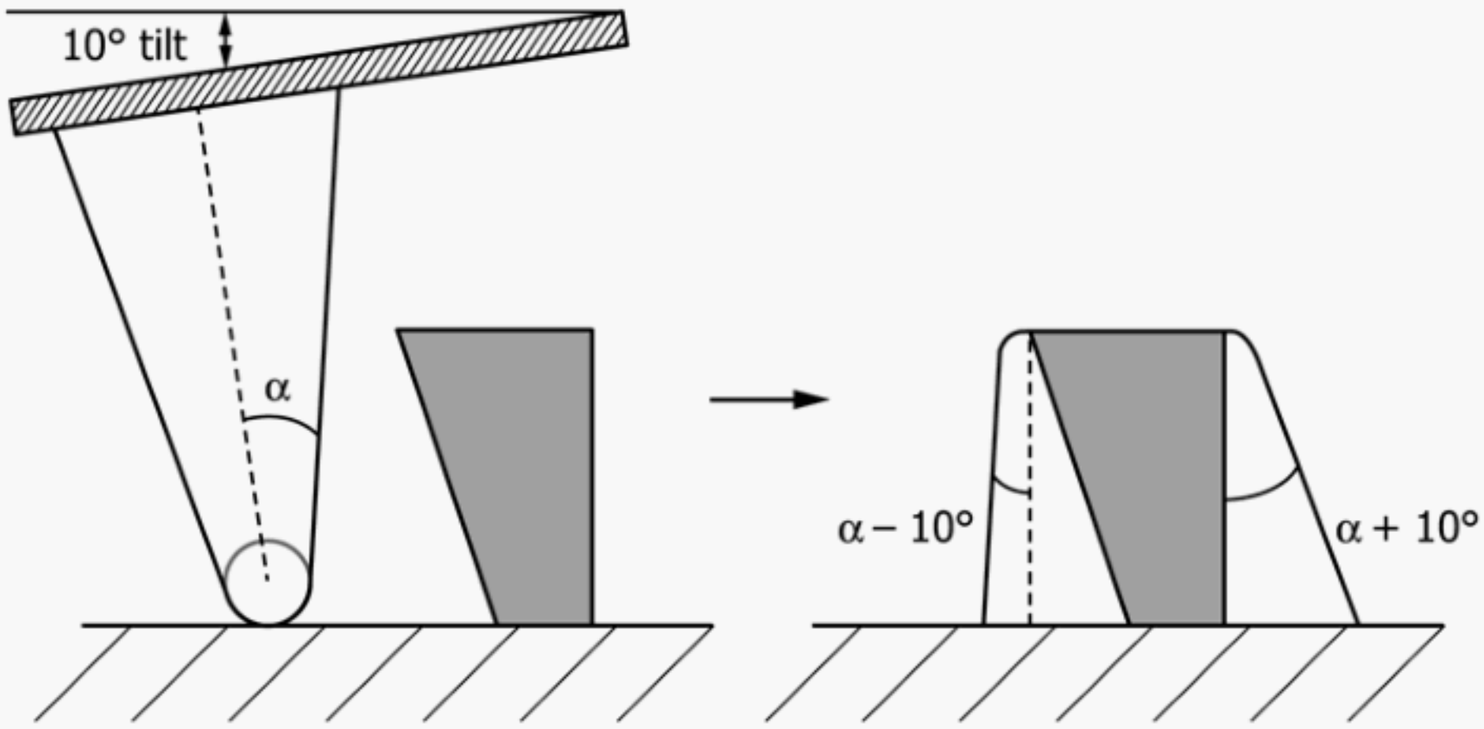

NOTE 1—Compare to Fig. 9.

FIG. 17 Schematic of the Effect of Changing the Tip *z*-axis on Image Broadening due to a Surface Feature which is Undercut

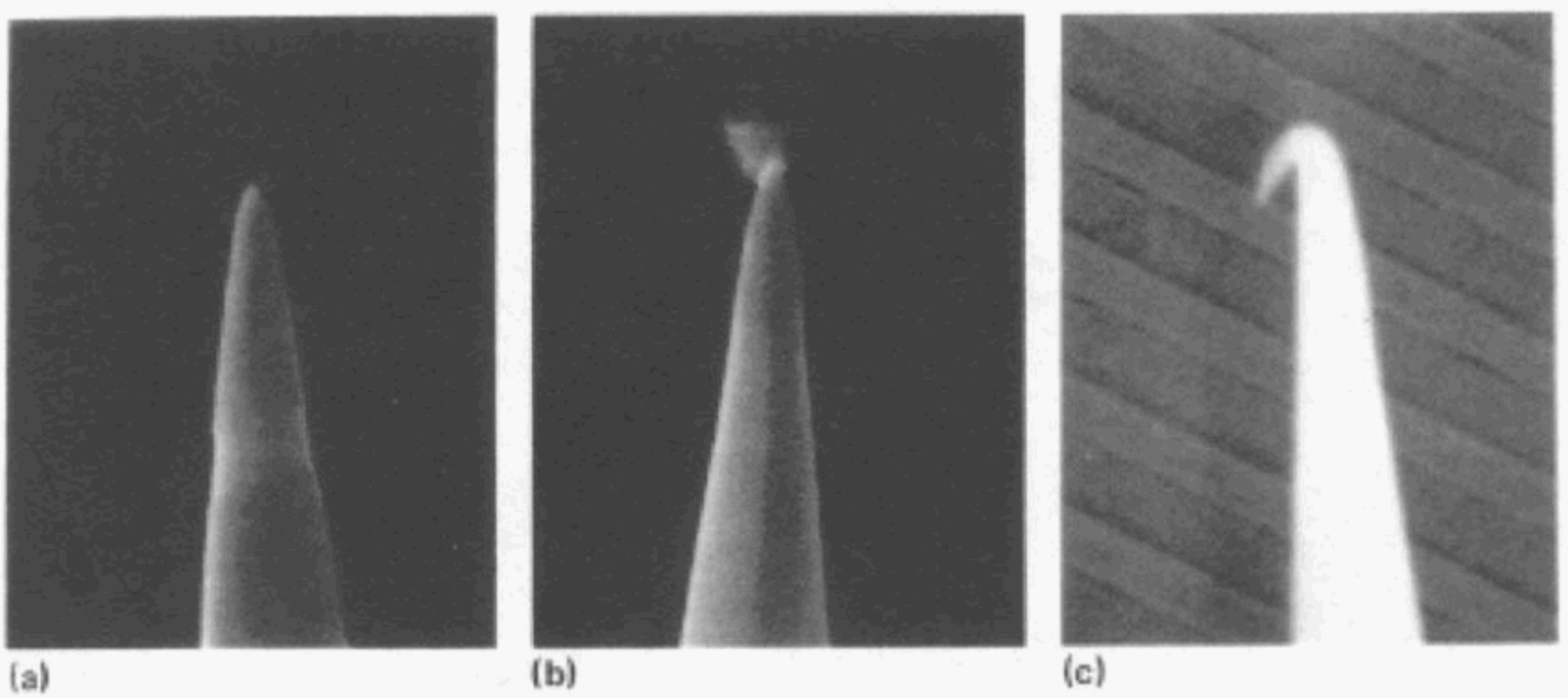

NOTE 1—The corresponding STM images generated by each tip are shown. In this example distortions are seen due to extrinsic effects, either tip contamination or tip damage with use. Although actual dimensions of the tips and line features are not indicated, the effect of tip shape on the resultant images is clearly demonstrated. (Used with permission of Hitachi, Ltd.)

FIG. 18 In-Situ SEM Micrographs of STM Tips Used to Scan a Test Line Structures

Copyright by ASTM Int'l (all rights reserved); Fri Jan 8 20:56:38 EST 2021

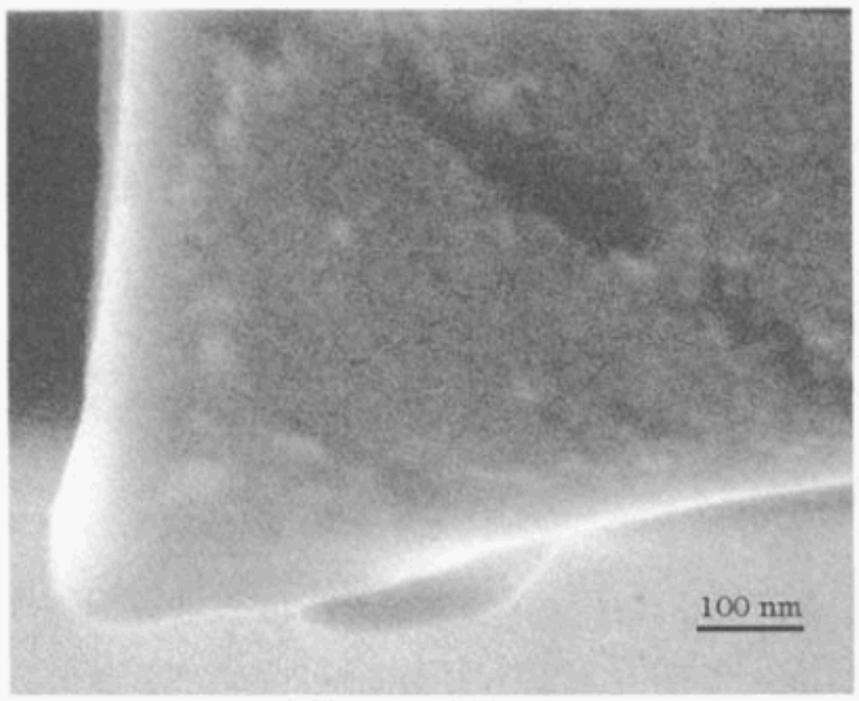

(a) a good tip

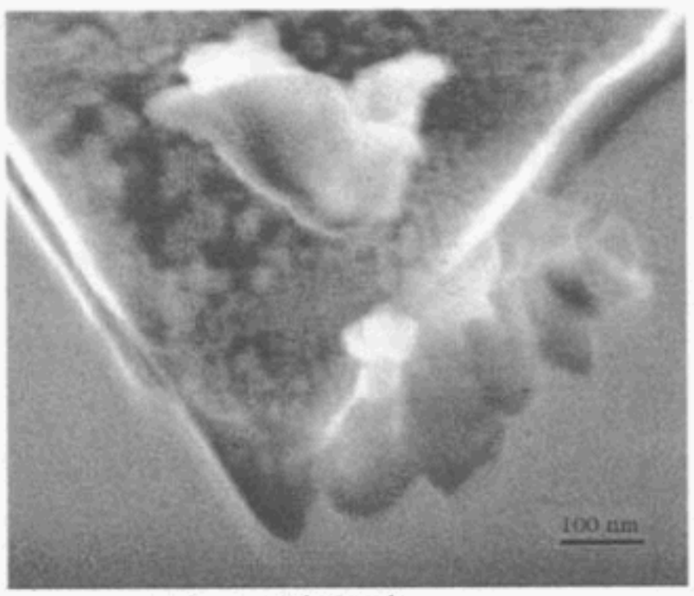

(b) multiple tip

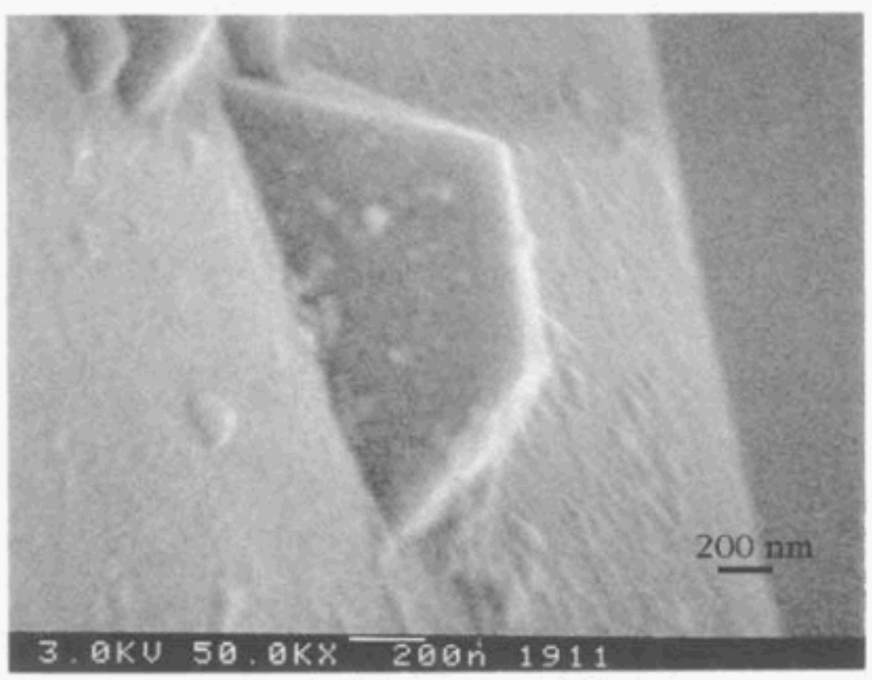

(c) truncated wedge

NOTE 1—In (***a***) a good tip is shown with a tip radius of curvature of about 40 nm. In (***b***) structural defects near the apex give rise to multiple tip images. In (***c***) non-uniform processing gives rise to a severely truncated pyramid. All three tips were obtained from the same wafer substrate. (Images courtesy of J. Blackson. Used with permission of The Dow Chemical Company.)

FIG. 19 FEGSEM Images of Typical Defects Found on Silicon Nitride AFM Tips

Copyright by ASTM Int'l (all rights reserved); Fri Jan 8 20:56:38 EST 2021

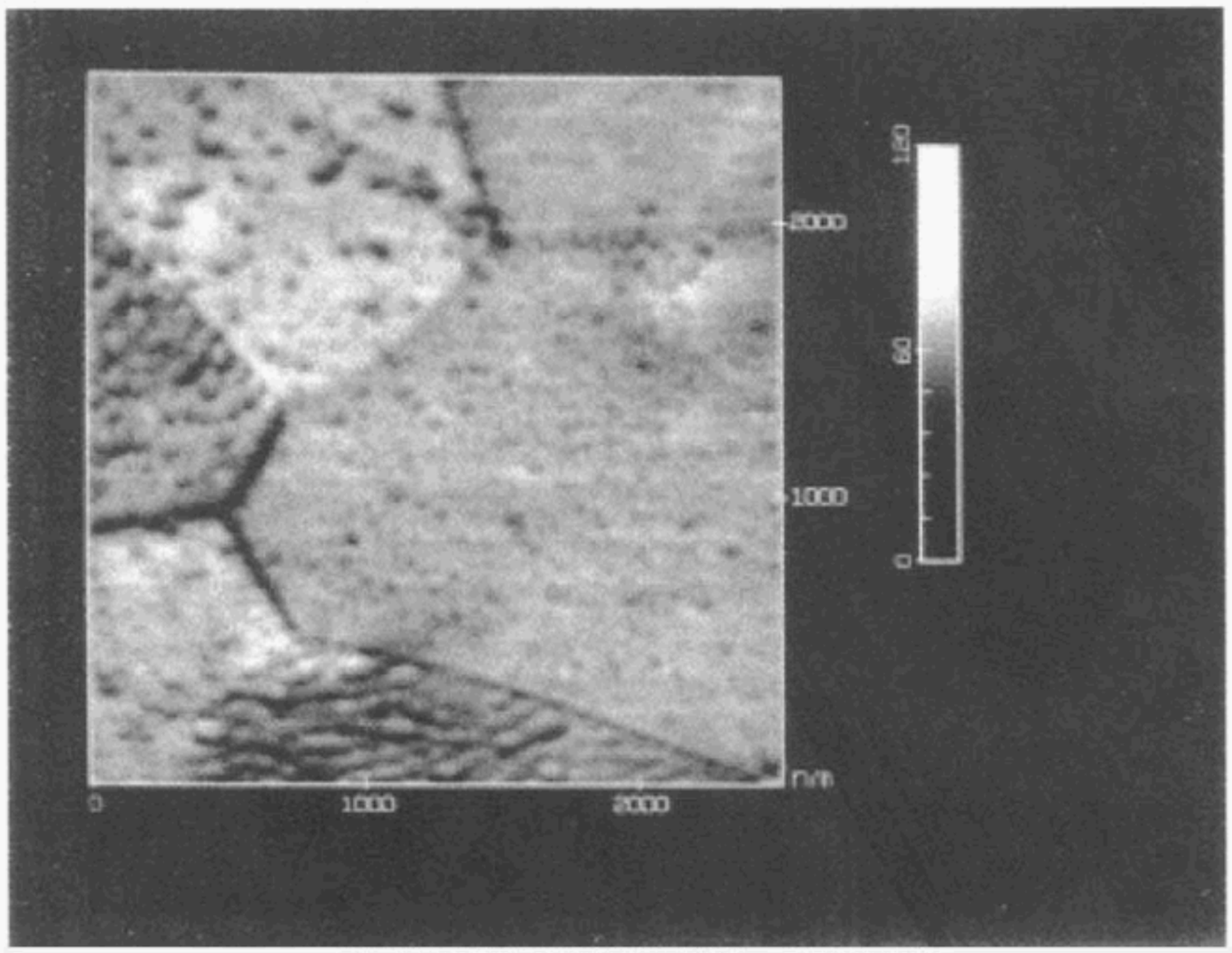

(A) IMAGE OBTAINED WITH A GOOD TIP

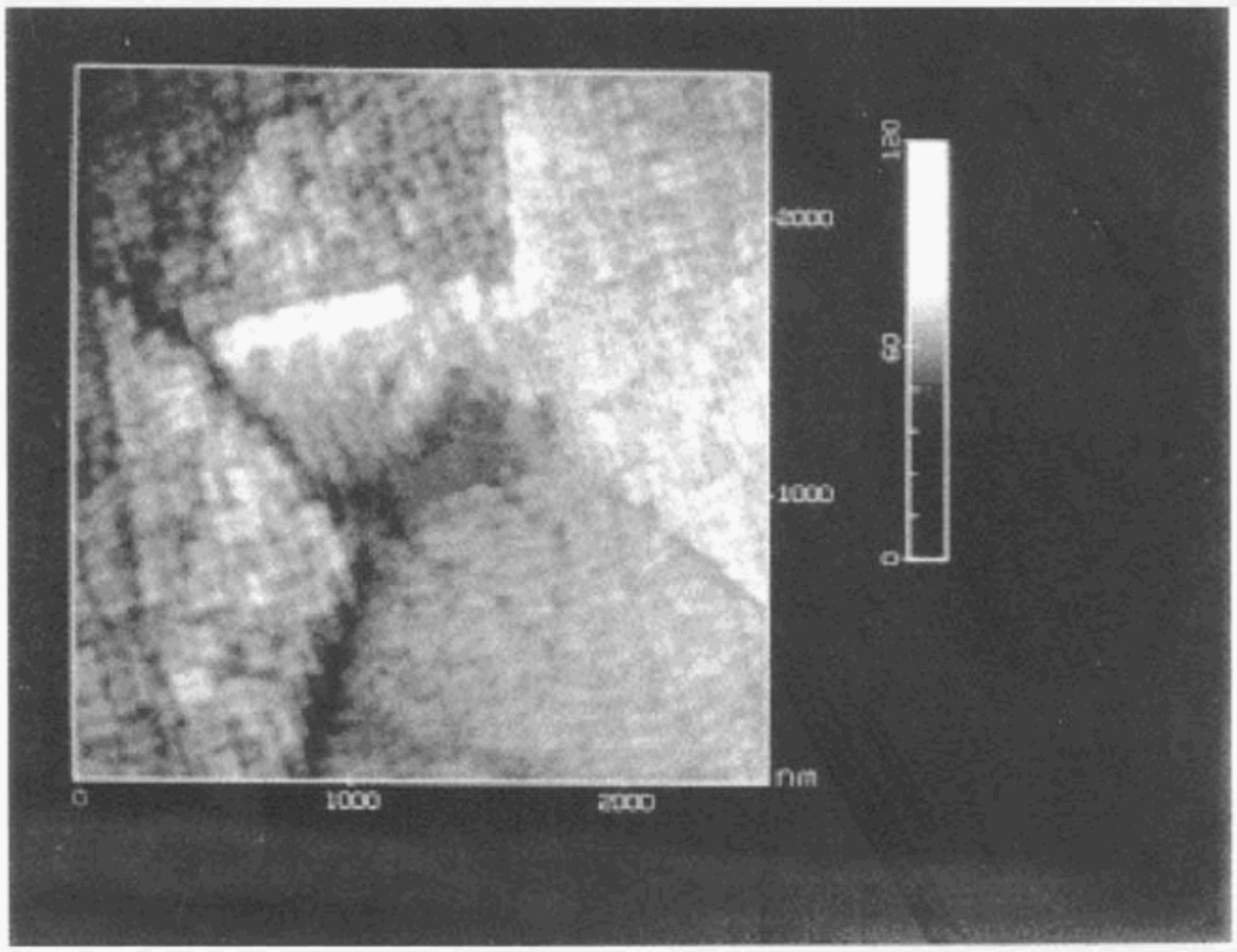

(B) IMAGE OBTAINED WITH A MULTIPLE TIP

NOTE 1—With a good tip, the image provides good detail of the grain structure (top). With a multiple tip like that of Figure 19b, the image has a "ghosted" appearance due to multiple contact points during imaging (bottom). (Images courtesy of G. Meyers. Used with permission of The Dow Chemical Company.)

FIG. 20 Example of a Multiple Tip Effect in the AFM Image of an Ion Sputtered Ceramic Surface

Copyright by ASTM Int'l (all rights reserved); Fri Jan 8 20:56:38 EST 2021

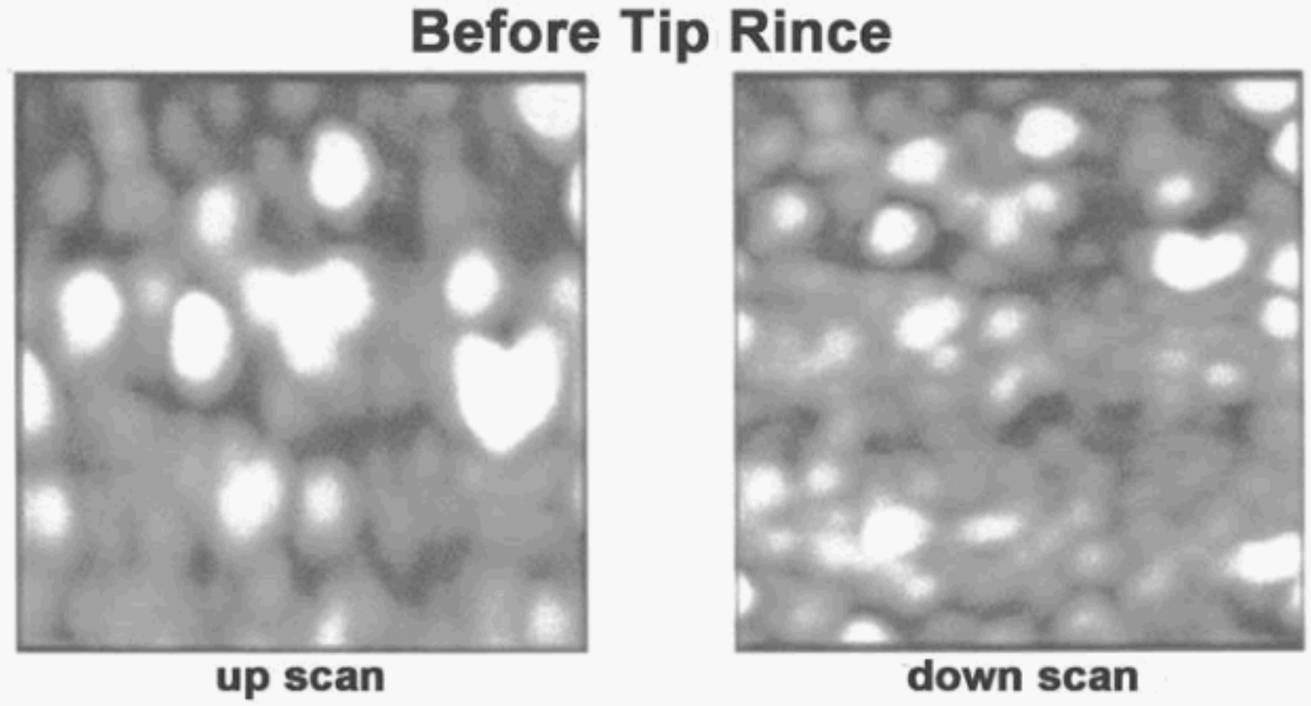

NOTE 1—These 500 nm × 500 nm topview images of a sputtered metal oxide surface showed reproducible distortions in the up and down scan directions. After cleaning the tip in methanol, the image quality improved and the up and down scans were now identical. (Images courtesy of G. Meyers. Used with permission of The Dow Chemical Company.)

FIG. 21 Example of Contamination Removal From a Tip

REFERENCES

(1) van de Leemput, L.E.C., Rongen, P.H.H., Timmerman, B.H., and van Kempen, H., *Review of Scientific Instruments*, Vol 62, No. 4, 1991, p. 989.

(2) Howland, R.S., *Atomic Force Microscopy/Scanning Tunneling Microscopy*, S.H. Cohen, M.T. Bray, and M.L. Lightbody, eds., Plenum Press, New York, 1994, pp. 347.

(3) Hues, S.M., Draper, C.F., Lee, K.P., and Colton, R.J., *Review of Scientific Instruments*, Vol 65, No. 5, 1994, p. 1561.

(4) Fu, J. *Review of Scientific Instruments*, Vol 66, No. 7, 1995 , p. 3785.

(5) Griffith, J.E., and Grigg, D.A., *Journal of Applied Physics*, Vol 74, 1993, pp. R83–R109.

(6) Snevity, D., and Vancso, J., *Langmuir*, Vol 9, No. 9, 1993, p. 2253.

(7) Schwarz, U.D., Haefke, H., Reimann, P., and Guntherodt, H.-J., *Journal of Microscopy*, Vol 173, No. 3, 1994, p. 183.

(8) Montelius, L., Tegenfeldt, J.O., *Applied Physics Letters*, Vol 62, No. 21, 1993, p. 2628.

(9) Reiss, G., Schneider, F., Vancea, J., and Hoffman, H., *Applied Physics Letters*, Vol 57, No. 9, 1990, p. 867.

(10) Keller, D., *Surface Science*, Vol 235, 1991, p. 353.

(11) Villarrubia, J.S., *Surface Science*, Vol 321, 1994, p. 287.

(12) Villarrubia, J.S., *Journal of Research of NIST* , Vol 102, 1997, p. 425.

(13) Thundat, T., Zheng, X.-Y., Sharp, S.L., Allison, D.P., Warmack, R.J., Joy, D.C., and Ferrell, T.L., *Scanning Microscopy*, Vol 6, No. 4, 1992, p. 903.

(14) Westra, K.L., and Thompson, D.J., *Journal of Vacuum Science and Technology B*, Vol 12, No. 6, 1994, p. 3176.

(15) Butt, H.-J., Guckenberger, R., and Rabe, J.P., *Ultramicroscopy*, Vol 46, 1992, p. 375.

(16) Martin, D.C., Ojeda, J.R., Anderson, J.P., and Pingali G., *Atomic Force Microscopy/Scanning Tunneling Microscopy*, S.H. Cohen, M.T. Bray, and M.L. Lightbody, eds., Plenum Press, New York, 1994, p. 217.

(17) Gallarda, H., and Jain, R., "Proceedings of Conference on Integrated Circuit Metrology, Inspection, and Process Control, V," *SPIE*, Vol 1464, 1991, p. 459.

(18) Pingali, G.S., and Jain, R., *Proceedings IEEE Workshop on Applications of Computer Vision*, 1992, p. 282.

(19) Vesenka, J., Manne, S., Giberson, R., Marsh, T., and Henderson, E., *Biophysical Journal*, Vol 65, 1993, p. 992.

Copyright by ASTM Int'l (all rights reserved); Fri Jan 8 20:56:38 EST 2021

(20) Xu, S., and Arnsdorf, M.F., *Journal of Microscopy*, Vol 173, No. 3, 1994, p. 199.
(21) Odin, C., and Aime, J.P., *Surface Science* , Vol 317, No. 3, 1994, p. 321.
(22) Allen, M.J., Hud, N.V., Balooch, M., Tench, R.J., Siekhaus, W.J., and Balhorn, R., *Ultramicroscopy* , Vol 42, 1992, p. 1095.
(23) Markiewicz, P., and Goh, C., *Langmuir*, Vol 10, 1994, p. 5.
(24) Keller, D.J., and Francke, F.S., *Surface Science* , Vol 294, 1993, p. 409.
(25) Bonnet, N., Dongmo, S., Vautrot, P., and Troyon, M., *Microscopy Microanalysis Microstructures*, Vol 5, 1994, p. 477.
(26) Wilson, D.L., Kump, K.S., Eppell, S.J., and Marchant, R.E., *Langmuir*, Vol 11, 1995, p 265.
(27) Williams, P.M., Shakesheff, K.M., Davies, M.C., Jackson, D.E., Roberts, C.J., and Tendler, S.J.B., *Journal of Vacuum Science and Technology B*, Vol 14, 1996, p. 1557.
(28) Villarrubia, J.S., *Journal of Vacuum Science and Technology B*, Vol 14, 1996, p. 1518.
(29) Dongmo, S., Troyon, M., Vautrot, P., Delain, E., and Bonnet, N., *Journal of Vacuum Science and Technology B* , Vol 14, 1996, p. 1552.

ASTM International takes no position respecting the validity of any patent rights asserted in connection with any item mentioned in this standard. Users of this standard are expressly advised that determination of the validity of any such patent rights, and the risk of infringement of such rights, are entirely their own responsibility.

This standard is subject to revision at any time by the responsible technical committee and must be reviewed every five years and if not revised, either reapproved or withdrawn. Your comments are invited either for revision of this standard or for additional standards and should be addressed to ASTM International Headquarters. Your comments will receive careful consideration at a meeting of the responsible technical committee, which you may attend. If you feel that your comments have not received a fair hearing you should make your views known to the ASTM Committee on Standards, at the address shown below.

This standard is copyrighted by ASTM International, 100 Barr Harbor Drive, PO Box C700, West Conshohocken, PA 19428-2959, United States. Individual reprints (single or multiple copies) of this standard may be obtained by contacting ASTM at the above address or at 610-832-9585 (phone), 610-832-9555 (fax), or service@astm.org (e-mail); or through the ASTM website (www.astm.org). Permission rights to photocopy the standard may also be secured from the Copyright Clearance Center, 222 Rosewood Drive, Danvers, MA 01923, Tel: (978) 646-2600; http://www.copyright.com/

Copyright by ASTM Int'l (all rights reserved); Fri Jan 8 20:56:38 EST 2021